ELSEVIER

Tectonophysics 325 (2000) 257–277

TECTONOPHYSICS

www.elsevier.com/locate/tecto

Synchronous magmatic cycles during the fragmentation of Gondwana: radiometric ages from the Levant and other provinces

Amit Segev *

Geological Survey of Israel, 30 Malkhe Israel Street, Jerusalem 95501, Israel

Received 22 January 1999; accepted for publication 12 May 2000

Abstract

Reliable and acceptable radiometric ages (mainly $^{40}Ar/^{39}Ar$) of igneous whole rocks from the Levant, representing non-orogenic igneous provinces, together with six igneous provinces of Gondwana, reveal 17 synchronous global magmatic events, including flood basalts. Their starting ages in the course of the last 205 million years (in Ma) are: 202, 190, 184, 169, 160, 145, 138, 125, 112, 97, 83, 69, 56, 44, 32, 17 and 5. The chronology of these events in Gondwana igneous provinces points to short-term magmatic cycles, consisting of magmatic events plus intermagmatic intervals, with an average duration of ca 13 m.y. The suggested synchronous events, which conform to geological periods and stage boundaries, probably reflect cycles of high-rate upper mantle upwellings that played a major role in the periodic ascent of melts across the lithosphere. The common geodynamic evolution of Gondwana igneous provinces was extension of the continental lithosphere, thinning, uplifting, breakup, massive igneous activity, spreading and drifting. All these provinces were affected by upwelling of lower mantle thermal anomalies. The chronology of magmatic events in each igneous province, which extended over thousands of kilometers and includes the plume provinces, suggests that the life-span (magmatic period) of these provinces averages 58 m.y., and in many cases, the first-term magmatic cycles are longer (11–17 m.y.) and more intensive.

The periodic magmatism, which followed the breakup and dispersal of Gondwana, suggests an evolutionary scenario for the development of oceanic spreading centers by the ascent of one or more (coexisting) large plume heads across the upper mantle.

Keywords: geochronology; Gondwana; Israel; periodicity; plumes; volcanic fields

1. Introduction

Since the Early Mesozoic, several igneous events have occurred in the Levant (Fig. 1). Igneous rocks are distributed over an area of ca 150×500 km in outcrops and the subsurface of Syria, Lebanon, Israel, Jordan and Sinai, comprising various volcanic sequences and small hypabyssalic intrusions. Contemporaneous magmatic activity is known from adjacent areas, such as the Arabian Peninsula (Sebai et al., 1991a; Zumbo et al., 1995a; Baker et al. 1996) and NE Africa (Egypt, Libya, Sudan, Ethiopia) (Cahen et al., 1984; Ebinger et al., 1993; Zumbo et al., 1995b; Hofmann et al., 1997; George et al., 1998; Wilson and Guiraud, 1998). Basalts ranging in composition from weakly sub-alkaline to alkaline are the dominant rock type, together with nephelin-

* Fax: +972-2-5380688.
E-mail address: segev@mail.gsi.gov.il (A. Segev)

0040-1951/00/$ - see front matter
PII: S0040-1951(00)00122-0

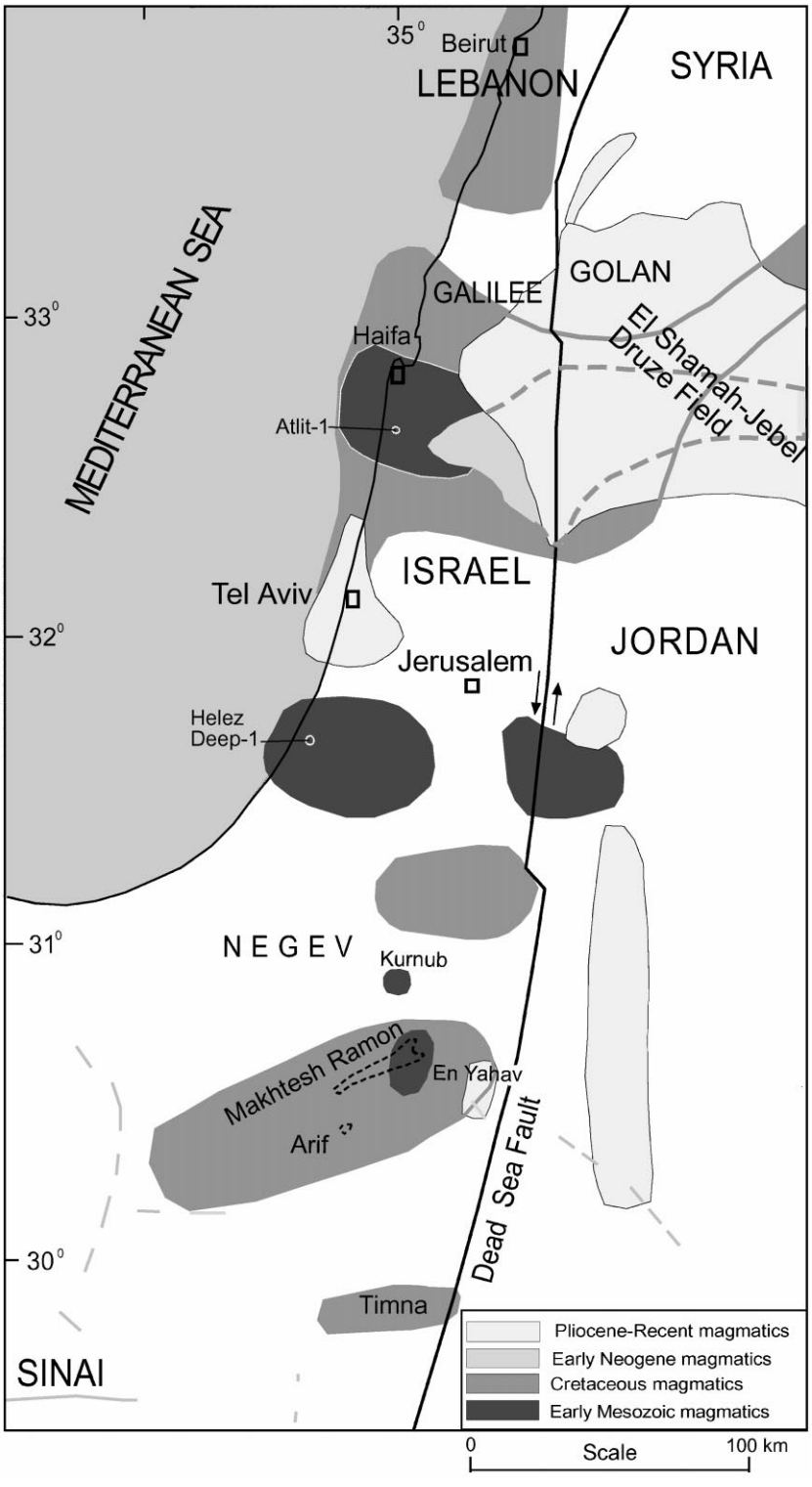
35°
Beirut
LEBANON
SYRIA
MEDITERRANEAN SEA
GALILEE
GOLAN
El Shamah-Jebel Druze Field
33°
Haifa
Atlit-1
ISRAEL
Tel Aviv
32°
JORDAN
Jerusalem
Helez Deep-1
NEGEV
31°
Kurnub
Makhtesh Ramon
En Yahav
Arif
Dead Sea Fault
30°
Timna
SINAI
Pliocene-Recent magmatics
Early Neogene magmatics
Cretaceous magmatics
Early Mesozoic magmatics
0
Scale
100 km

ites, basanites, micro-gabbros, quartz-syenites and trachytes (Stein and Hofmann, 1992), all enriched in incompatible elements (e.g. LREE) and related to rifting and hot spots or mantle plumes (Garfunkel, 1989; Stein and Hofmann, 1992, 1994; Wilson and Guiraud, 1998). These commonly caused doming ~1–2 km above the surrounding surface with subsequent thinning and fracturing of the lithosphere.

Widespread igneous occurrences are crustal emplacements of predominantly ferromagnesian extrusive and intrusive rocks that originated in mantle plume processes (Coffin and Eldholm, 1994). Initially, the term plume was used for hot buoyant material rising from the mantle, creating volcanoes or hotspots such as Iceland and Hawaii (e.g. Morgan, 1971, 1981; Vogt, 1972), and was modeled as having a mushroom-shaped head about 100 km in diameter (Turcotte and Schubert, 1982; Ribe and Christensen, 1994) and a narrow cylindrical tail. The model of Griffiths and Campbell (1990), however, predicts that a plume head derived from a deep mantle source (2800 km) attains a diameter of 800–1200 km. Furthermore, plumes also refer to larger (thousands of kilometers) mantle convection cells with ascending hot material being displaced by descending cold material (Turcotte and Schubert, 1982; White and McKenzie, 1989). In the present paper, the term plume refers to the upwelling of a large-scale mantle convection cell (approximately thousands of kilometers in size), and the term igneous province is the overall area where extrusive (commonly in enormous quantities) and intrusive activity took place. The area where the igneous rocks have a plume signature is the plume province. Laboratory experiments on the lateral extension and flattening of a plume head beneath the lithosphere, after the time of maximum uplift, suggest that this extension and flattening continues for at least 20 m.y. (Griffiths et al., 1989). This time span is slightly shorter than the magmatic periods defined in the Levant.

The above-mentioned deep mantle plume theory has gained widespread acceptance in the literature (Kent, 1994), although other models, such as 'convective partial melting' (Mutter et al., 1988) or 'plate tectonic reorganization' (Anderson, 1994a,b) have been suggested for the origin of continental flood volcanics (CFVs) and other igneous provinces.

The stratigraphic evidence and isotopic age determinations (K/Ar from Lang et al., 1988; Lang and Steinitz, 1989; Recanati et al., 1989; and Rb/Sr from Steinitz, 1980; Lang et al., 1988) indicate that igneous activity began in Early Mesozoic times and continued episodically until the Senonian (Lang et al., 1988; Lang and Steinitz, 1989). Following a quiescence of several tens of million years, magmatic activity resumed during the Miocene (Steinitz et al., 1978), and continued up to subrecent times (Mor, 1986; Heimann et al., 1996). Due mainly to analytical problems, earlier interpretations of whole-rock (WR) K/Ar and Rb/Sr data revealed broad ranges of magmatic activity, and the duration of events thus remained uncertain. By applying the $^{40}Ar/^{39}Ar$ dating technique to some of the WR samples (Kohn et al., 1993; Lang and Steinitz, 1994, 1996; Heimann et al., 1996), the range of the K–Ar dates became significantly constrained, but still did not establish a reliable time interval for specific magmatic events.

The present paper summarizes new mainly reliable radiometric data from T. Weissbrod, A. Segev and Y. Kapusta, Y. Kolodny and H. Ron, M. McWilliams and H. Ron, Z. Lewy, B. Lang and A. Segev (unpublished), adds reinterpreted $^{40}Ar/^{39}Ar$ WR dates from Heimann (1990), Kohn et al. (1993), Lang and Steinitz (1994), Lang and Steinitz (1996), Baer et al. (1995), Teutsch et al. (1996) and Heimann et al. (1996), together with a few valid Rb/Sr results from Steinitz (1980) and Lang et al. (1988), mainly from Israel, and reveals 13 magmatic events in the Levant area during the past 245 m.y. These magmatic events are correlated with available reliable and accepted geochronological data (mainly $^{40}Ar/^{39}Ar$, Rb/Sr and U/Pb results) of magmatic events along the dispersed provinces of Gondwana (central and southern Atlantic Ocean, Indian Ocean, Karoo, Marie Byrd Land-Eastern Australia and Balleny).

The synthesis of the above-mentioned geochronological data enables the hypothesis of 'global

Fig. 1. Location map and distribution of Mesozoic–Recent magmatic rocks in Israel and adjacent areas. The magmatic fields east of the Dead Sea Fault are restored to their pre-strike-slip location (modified after Garfunkel, 1989).

synchronous magmatic episodes' to be tested and sheds light on the evolution of a lower mantle plume head.

2. Methods

Most of the samples for $^{40}Ar/^{39}Ar$ dating from Israel were prepared at the Geological Survey of Israel (GSI) laboratories and were irradiated in the IRR-1 reactor at the Soreq Nuclear Center, Israel (Heimann et al., 1992). Of the published results (see Table A1 in Appendix A), 22 samples remain unchanged, 16 were reinterpreted, and five samples from Weissbrod, Segev and Kapusta have not yet been published. The samples were fused by inductive furnace and analyzed by an MM-1200B mass spectrometer at the GSI geochronological laboratory (and were described in detail by each of the authors quoted). Corrections for the irradiation parameter, *J*, were done using the LP-6 standard (with an assumed age of 128.5 Ma; Roddick, 1983) for Kohn et al. (1993), Lang and Steinitz (1994, 1996), Baer et al. (1995), Weissbrod, Segev and Kapusta (unpublished), and HD-B1 (assumed age of 24.7 Ma, Führmann et al., 1986) for Heimann (1990) and Heimann et al. (1996). Representative spectra are shown in Fig. 2a–m.

Ten additional $^{40}Ar/^{39}Ar$ analyses of WR basalt samples were carried out at Stanford University (Kolodny and Ron, unpublished; McWilliams and Ron, unpublished; Appendix A, Fig. 2n–q). The samples were irradiated at the USGS TRIGA reactor in Denver. The argon was extracted in a vacuum furnace and analyzed with a MAP 216 mass spectrometer (Teutsch et al., 1996). Corrections for the irradiation parameter, *J*, were made using the Taylor Creek sanidine standard (85G003 with an assumed age of 27.92 Ma; Izett et al., 1991).

The potassium, for conventional K–Ar measurements of hornblende xenocrysts (Lewy, Lang and Segev, unpublished; see Appendix B), was determined after fusing with $Li_2B_2O_4$ by ICP-AES (Perkin Elmer Optima 3000), and Ar measurements were carried out at the GSI geochronological laboratory using the standard isotope dilution procedure (MM-1200B mass spectrometer) (Lang et al., 1988; Lang and Steinitz, 1989).

Selected samples for refinement of their $^{40}Ar/^{39}Ar$ age spectra were first evaluated as to their suitability for age interpretation. In flat spectra, the calculated 'plateau' and near 'plateau' age (containing three or more steps that are all statistically equivalent at the 2σ level, and their weighted mean age containing $>50\%$ of the ^{39}Ar released) were considered as the true age (discussed in detail by Baksi, 1999). Weighted mean ages of $<50\%$ released ^{39}Ar were adopted as best estimate ages (or 'marginl plateau') by applying the following criteria (e.g. Baker et al., 1996):

1. For decreasing apparent age spectra (from low-*T* to high-*T*): the high-*T* steps are accepted as a true age when they are only slightly disturbed, and continue to the end (mainly effects of ^{39}Ar deficit; see Fig. 2d and q); or in cases with Ar recoil/redistribution of highly disturbed decreased apparent age spectra (much older dates at low-*T* steps and very young dates at high-*T* steps; see Fig. 2g and h), the relatively flat part of the spectra (before a sharp declined step), commonly between 800–950°C, is accepted as a true age, considering the suggestion of Baksi (1999).
2. Step-age minima in least disturbed saddle-shaped spectra (Fig. 2e) is accepted as a 'maximum' age.
3. Step-age maxima (advisably two or more continuous steps having approximately 40% of the total ^{39}Ar) in strong Ar loss spectra (Fig. 2j) is accepted as an estimated age.
4. In more complex age spectra, several criteria should be applied (Fig. 2c, i, and j).

3. New and reinterpreted $^{40}Ar/^{39}Ar$ and K/Ar ages of Mesozoic–Cenozoic igneous rocks in Israel

A list of published (part of them reinterpreted) $^{40}Ar/^{39}Ar$ WR and mineral ages (including unpublished data from Weissbrod, Segev and Kapusta, Fig. 2m) of magmatic rocks in Israel is given in Appendix A and Fig. 2. Unpublished data from Kolodny and Ron, and McWilliams and Ron are given in Appendix B, Fig. 2n–q, and from Lewy, Lang and Segev in Table C1 (Appendix C).

The refinement of the 16 disturbed WR igneous samples yields differences of up to 4% from the

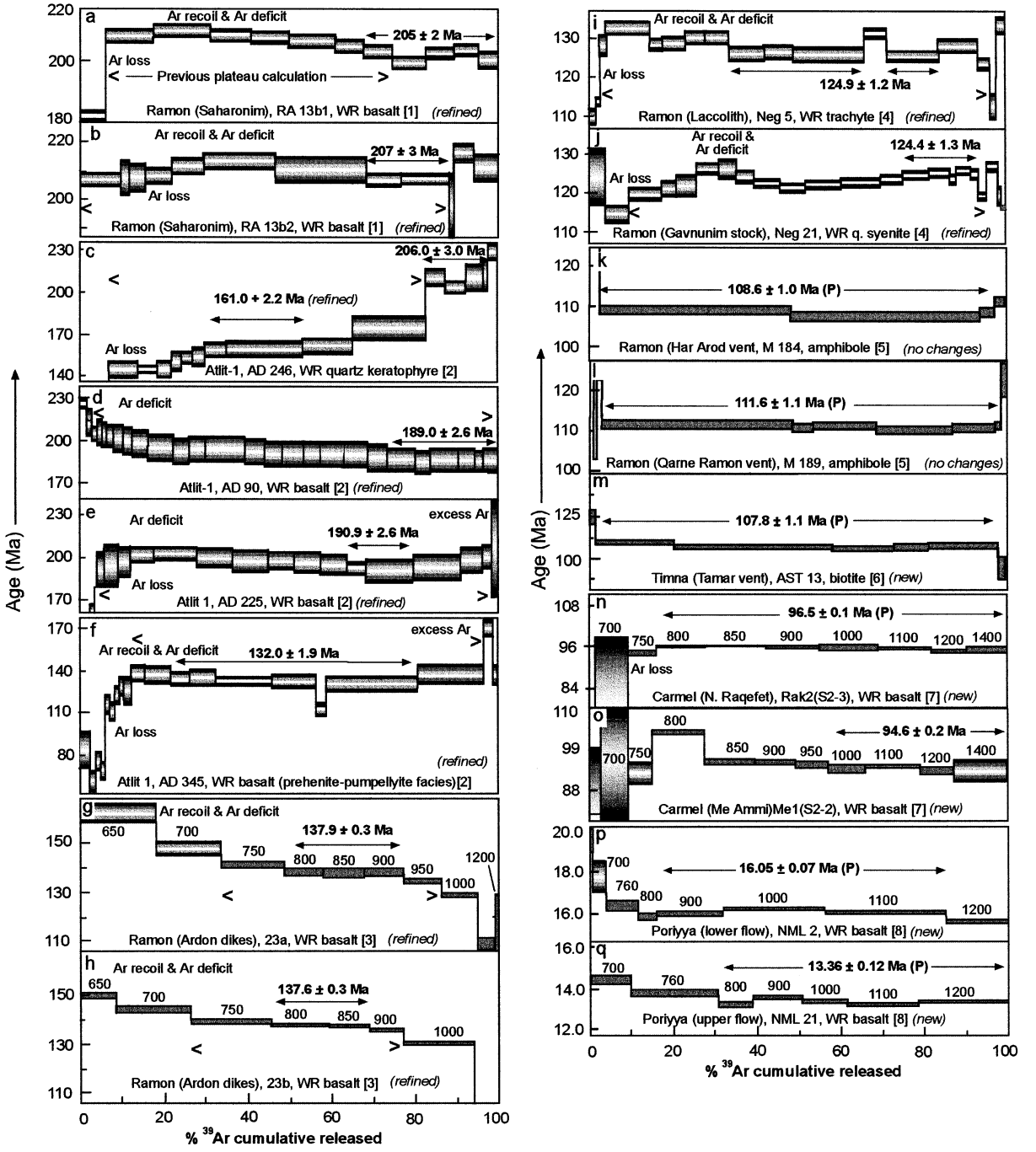

Fig. 2. Selected $^{40}Ar/^{39}Ar$ age spectra for most of the Levant magmatic events (the height of the boxes indicates analytical errors of $\pm 1\sigma$ about each step) (P: plateau age). Sources: 1: Baer et al. (1995); 2: Kohn et al. (1993); 3: Teutsch et al. (1996); 4: Lang and Steinitz (1994); 5: Lang and Steinitz (1996); 6: Weissbrod, Segev and Kapusta (unpublished, Appendix A); 7: Kolodny and Ron (unpublished, Table B1 in Appendix B); 8: McWilliams and Ron (unpublished, Appendix B).

published $^{40}Ar/^{39}Ar$ ages, which decrease the range of dates of the magmatic events, thus enabling differentiation among them and estimates of inter-magmatic intervals. The fine-grained WR volcanic materials usually show a $^{40}Ar/^{39}Ar$ apparent age spectrum that has been subjected to natural and artificial effects that cannot be quantified. These are ^{40}Ar loss [decrease of spectra at the low-temperature (T) steps], excess ^{40}Ar (raising the spectra, commonly at high-T steps), ^{39}Ar plus ^{37}Ar loss and redistribution caused by recoil in the nuclear reactor (Turner and Cadogan, 1974; Huneke and Smith, 1976), together with ^{39}Ar deficit caused by the presence of water in the sample, which yields a significantly higher date at the low-T steps (Kapusta et al., 1994). The main problem is the interference of two opposing effects — Ar recoil/redistribution plus Ar deficit (Fig. 2d, g, h, p, and q) versus Ar loss (Fig. 2a, b, f, j, and o) — at the low-temperature steps.

In addition to geological evidence, at least two $^{40}Ar/^{39}Ar$ ages, or a combination of one $^{40}Ar/^{39}Ar$ age accompanied by a Rb/Sr isochron age, are required to define a magmatic event. None of the precise GSI $^{40}Ar/^{39}Ar$ ages are rejected, except for two duplicate samples (Ra-13) of Early Jurassic age with an $^{40}Ar/^{39}Ar$ ratio >100 that was measured by MS10 mass spectrometer (in Liverpool, UK) having a small radius of curvature (Baksi, 1999). Both samples yielded dates of $\sim 3\%$ older than their GSI duplicates (Baer et al., 1995).

A summary of the new age ranges from Israel (data in Appendices A–C) and nearby countries (data in Table D1 in Appendix D, Afar province) is given in Table 1. The new data set of mainly $^{40}Ar/^{39}Ar$ ages indicates at least 13 magmatic events (Fig. 3) during the last 245 m.y. in the Levant and nearby regions (Segev, 1998). Of these events: four (J_3?, C_3, C_4, C_5) are new; five (J_1, J_2, C_1, C_2, T_3) are reinterpreted; and four (Tr, T_1, T_2, T–Q) are from the cited references. Furthermore, the individual systematic events can be grouped into three active magmatic periods, lasting 46 and 56 m.y., and quiescent intervals of ~ 30 m.y. (Fig. 3). At this stage, only the Cretaceous and Tertiary magmatic periods are well established in Israel, whereas the Jurassic and older magmatic periods are still in need of more radiometric measurements. The Tertiary magmatic period (the Afar Province) differs from earlier periods by

Table 1
Summary of new and reinterpreted age ranges of magmatic events in Israel and nearby countries (all ages are in million years, Ma)[a]

Magmatic event	Location of samples[b]	$^{40}Ar/^{39}Ar$ ages	Other ages
T–Q	Israel, Syria, Jordan, S.A.	5.1 ± 0.1–subrecent	
T_3	Galilee, Syria, Jordan	<13.4–16.0 ± 0.1	
T_2	Eth., Yem., S.A., Sinai, Negev	21.1–30.7 ± 0.2	
T_1	South Eth.	34.1–45.2 ± 1.4	
C_5	Carmel		83 ± 1.7[c]
C_4	Carmel, Lebanon, Syria	94.6–$>96.5 \pm 0.4$	
C_3	Negev, North Israel	108.1–111.6 ± 1.2	
C_2	Negev	124.4–124.9 ± 1.3	124 ± 13, 123 ± 9[d]
C_1	Negev, North Israel	132.0–137.9 ± 0.3	
J_3	Carmel	161 ± 2.2[e]	
J_2	Carmel	189.0–190.9 ± 2.6	
J_1	Negev, North Israel	205–207 ± 2.0	
Tr	Sinai, Negev, Central Israel	240 ± 4[f]	244 ± 44[d]

[a] For data and sources, see Appendices C and D. Tr: Triassic; J: Jurassic; C: Cretaceous; T: Tertiary; Q: Quaternary; Eth: Ethiopia; Yem: Yemen; S.A.: Saudi Arabia.

[b] Evidence of the Cretaceous events (only K–Ar data) is known also from Lebanon and Syria.

[c] New K/Ar data for hornblende separates (Appendix C).

[d] Rb/Sr data for acid igneous rocks.

[e] Age of low-grade metamorphism (one sample from the subsurface) representing heating by later cited magmatism.

[f] Unpublished spectra.

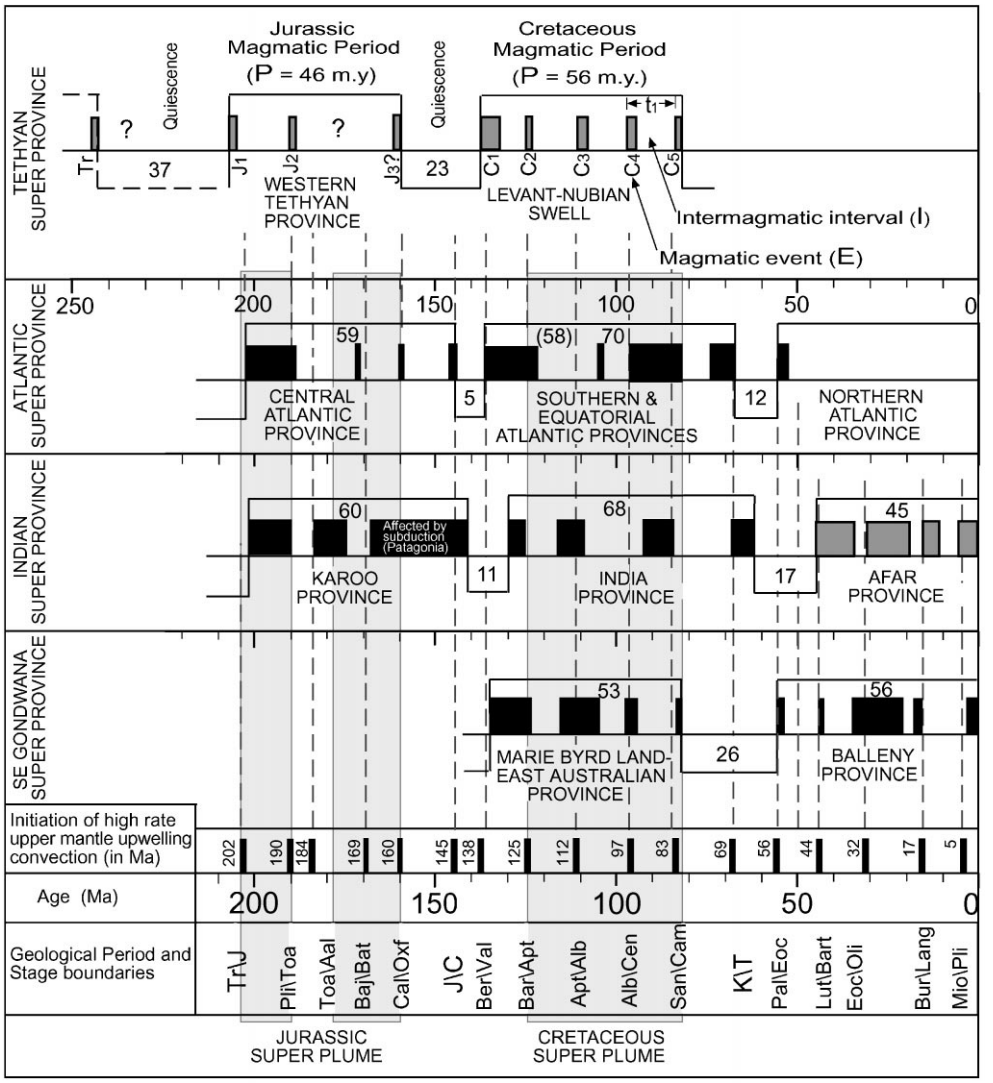

Fig. 3. Ages of the Levant magmatic events (gray color) as representative of the Tethyan Super province. Note the first-order (t_1) magmatic cycles. In addition, correlation between the ages of magmatic events within other provinces of Gondwana, the suggested intervals of high rate upper mantle upwelling convection (see Table 3), and the suggested intervals of super plumes are presented (Larson, 1991; Algeo, 1996) (for abbreviations, see Table 3).

its longer magmatic events and shorter intermagmatic intervals. These magmatic periods can be subdivided into short-term cycles (t_1, Fig. 3); a cycle consists of a magmatic event ($E=1$–3 m.y.) plus an intermagmatic interval ($I=\sim 12$ m.y., on average) lasting ($t_1=E+I$) approximately 13 m.y.

Within many of the magmatic periods, the initial events were both longer-lasting and more intensive than the following events (Table 1, Fig. 3). The present results point to an episodic (time-dependent) system for which the magmatic period represents the life-span of an igneous province.

In this context, the Jurassic magmatic period (between 205 and $\sim$161 Ma), known in the Levant mainly from the subsurface, is probably part of a large 'Western Tethyan Province' at the northern

part of Gondwana (Fig. 4), which is associated with the opening of the Neotethys (Sengör et al., 1984). Most of this province has been subducted under the Mediterranean convergent region. The younger Cretaceous magmatic period (between 138 and 83 m.y.) in the 'Levant-Nubian Province (Swell)' is presumably an eastern continuation of the Tethyan Ocean magmatic activity (Fig. 4). This small province was brought into juxtaposition with Eurasia by Cenozoic continental collision. These two igneous provinces with overlapping areal distributions, which, according to their geochemical evidence, relate to mantle plumes (Stein and Hofmann, 1992, 1994), were merged into the Tethyan super province (Fig. 4). Whereas both the Jurassic and the Cretaceous magmatic periods have fewer preserved igneous provinces (Segev, 1999), the Tertiary magmatic period (between 45 Ma and Recent), is a well-preserved province (the Afar) associated with the Afar plume (Schilling et al., 1992; Ebinger et al., 1993; Zeyen et al., 1997; George et al., 1998), which caused uplift, magmatism, breakup and drifting of the Afro-Arabian Plate.

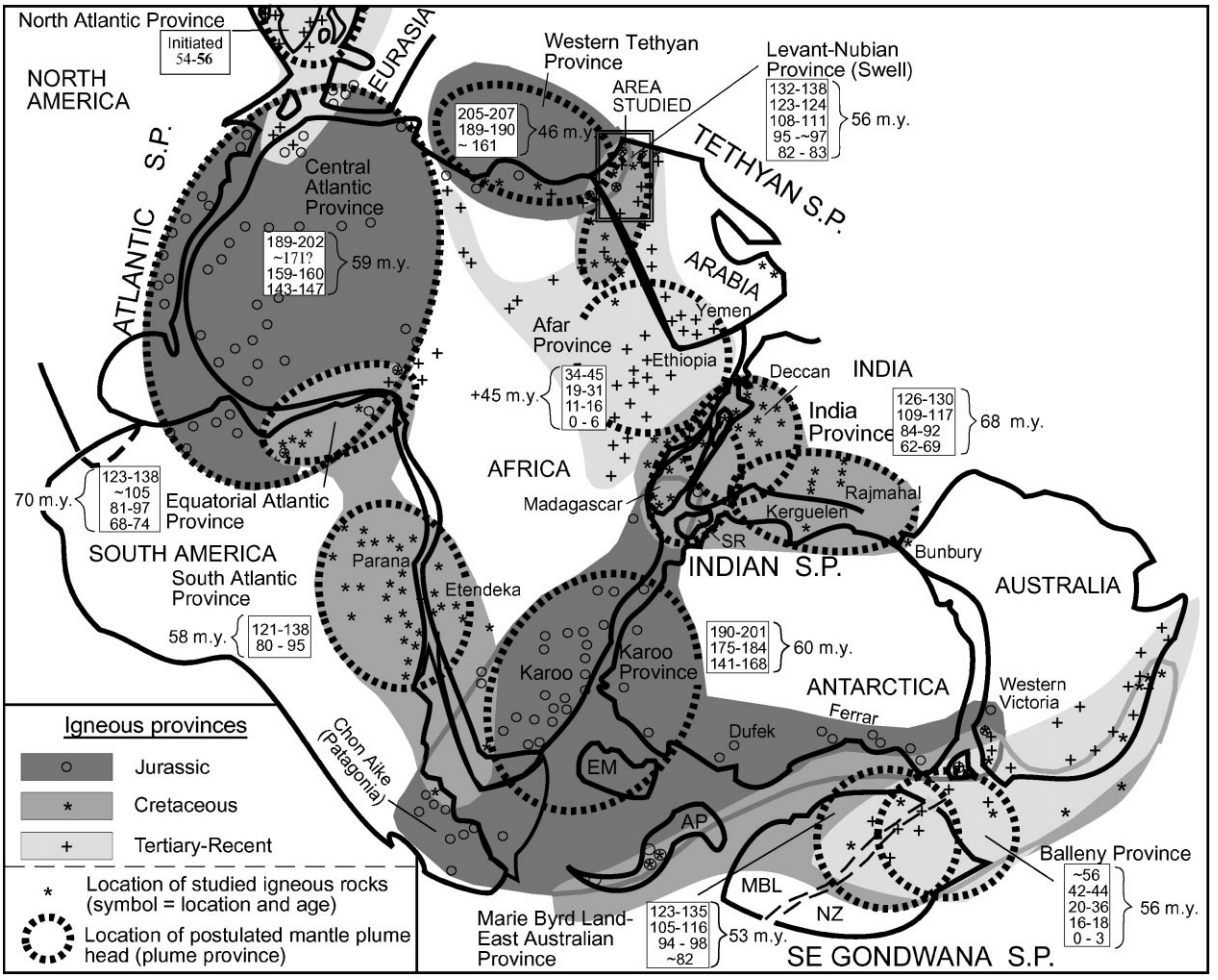

Fig. 4. Inferred distribution of igneous provinces, super provinces and mantle plume heads (plume provinces) within Gondwana. Note the location of the dated rocks and the ages of the magmatic events. The outlines of the continent's paleogeography during the Triassic (~ 220 m.y.) are mainly after Wilson et al. (1996). EM: Ellsworth Mountains; AP: Antarctic Peninsula; MD: Madagascar; SR: Sri Lanka; SEY: Seychelles; MBL: Marie Byrd Land; NZ: New Zealand.

4. Ages of Jurassic–Recent magmatic events in igneous provinces inside Gondwana

The Levant area represents a relatively limited part of the northern Gondwana super-continent, from which widespread magmatic occurrences are known from its drifted fragments.

Widespread igneous occurrences or events include crustal emplacements of predominantly ferromagnesian extrusive and intrusive rocks consisting mainly of continental flood volcanics (CFV) and non-orogenic complexes, passive margin volcanics and oceanic plateaus.

A series of magmatic events throughout a period and along a common continental breakup axis within Gondwana were grouped into nine provinces (including the Tethys) of spatial magmatic activity (Fig. 4). Like the above-mentioned Tethyan super province, igneous provinces from extensional environments with overlapping areal distributions are grouped into three additional super provinces. The following data set (Appendix D, Table 2, Fig. 4) includes the most recent partially selected Ar/Ar (a few K/Ar mineral separates ages from certain locations for a lack of better results), Rb/Sr and U/Pb radiometric ages of magmatic events (defined as above), but ignores continuous activity of hotspots and 'normal' mid-ocean ridges. Some of the continental magmatic provinces have been intensively studied (Central Atlantic, Karoo, Paraná-Etendeka, Deccan, Afar), and some are still based on mainly uncertain K/Ar dates (Marie Byrd Land-Eastern Australia and Balleny). The oceanic provinces commonly suffer from limited information.

The age ranges of the better-studied magmatic events may represent their realistic distribution, but those of the less-studied magmatic events could represent dispersion of ages as a result of analytical limitations.

5. Discussion and conclusions

Large parts of the igneous provinces described, particularly those with CFVs, were suggested to have formed by deep mantle plume activity, and the location of these postulated mantle plume heads are depicted on each of the igneous provinces (Fig. 4; after Cox, 1989; White and McKenzie, 1989; Schilling et al., 1992; Lanyon et al., 1993; Weaver et al., 1994; Wilson and Guiraud, 1998). Most of the igneous rocks within the plume provinces are geochemically characterized by a strong mantle signature.

A plot of the ages of Gondwana magmatic events (Fig. 3) demonstrates long-term periods similar to those in the Levant. The duration of eight magmatic periods (including the Tethyan super province and excluding the Afar province, which has not yet ended; Table 2) ranges between

Table 2
Summary of ages of magmatic events in the igneous provinces within Gondwana[a]

Igneous province	Length (km)	Magmatic events					Total duration
		I	II	III	IV	V	
Atlantic super province							
Central Atlantic	~5000	202–189	~171?	160–159	147–143		59
South Atlantic		138–121	95–80				58
Equatorial Atlantic		138–123	~105	97–81	74–68		70
Indian super province							
Karoo	~5500	201–190	184–175	168–141			60
India		130–126	117–110	92–84	69–62		68
Afar	>5000	45–34	31–19	16–11	6–0		45
SE Gondwana Sup. Pro.							
MBL-East Austr.	>5000	135–123	116–105	98–94	~82		53
Balleny	~4400	~56	44–42	36–20	18–16	3–0	56

[a] All ages are are in million years Ma. For sources and references see Appendix D.

53 and 70 m.y. (58 m.y. avg.). The spatial distribution (2000–5000 km), similar evolution and temporal behavior of the reviewed provinces, as well as the existence of plume heads within all of them (according to pro-plume advocates), suggest that they are the result of lower mantle convection (upwelling) or plumes initiated at the core–mantle boundary (Olson et al., 1990). The global synchronization for the initiation and termination of these magmatic periods is less conspicuous than the correlation of the initiation of magmatic events.

In several igneous provinces (central Atlantic, southern Atlantic, Karoo), as in the Levant, the internal distribution of magmatic events within the magmatic periods shows longer (~11–17 m.y.) and more intensive magmatism during the initial events, and the subsequent events tend to appear at the global synchronous intervals. The exceptionally long duration (168–141 m.y.) of the last magmatic event of the Karoo province (Patagonia and the Antarctic Peninsula) is probably due to the mixed environments — continental extention and subduction (reviewed by Féraud et al., 1999).

Data on global plume synchronism have been previously based on uncertain age determinations (Vogt, 1972) of low resolution and, therefore, with no possibility of separating between various events. Thus, world-wide synchronism of events could not be demonstrated. The Levant area, where cyclicity during the past 205 m.y. is based on reliable isotopic data and where the events are distinct, may be used as a datum to test for possible global synchronism.

The correlation adopted the starting ages of the magmatic events because the duration of each individual event is controlled by the plume and the local lithospheric characteristics. The described plume provinces of Gondwana reveal the following global synchronous magmatic events, in Ma

Table 3
Summary of the starting ages of magmatic events in four super provinces vs. time-scales of Harland et al. (1990) and Gradstein et al. (1995)[a]

Tethyan SP	Atlantic SP	Indian SP	SE Gond. SP	LIP	Most probable	STC	Time-scale[b]	
207	202	201			202	12	205.7±4.0	**Tr/J**
190					190	6	189.6±4.0	Pli/Toa
		184			184	15	180.1±2.6	Toa/Aal
	171	168			169	9	169.2±4.0	Baj/Bat
~161	160				160	15	159.4±3.6	Cal/Oxf
	147	145			145	7	144.2±2.6	**J/Cr**
138	138	130?	135		138	13	137.0±2.2	Ber/Val
124			125	Ont.–~124[c]	125	13	(121.0±1.4?)	Bar/Apt
111	~105	117	116		112	15	112.2±1.1	Apt/Alb
97	97	92	98		97	14	98.9±0.9	Alb/Cen
83			~82		83	14	83.5±0.5	San/Cam
	74	69			69	13	66.0±0.1	**Cr/T**
	56[d]		~56		56	12	56.5	*Pal/Eoc*
		45	44		44	12	42.1	Lut/Bart
		31	36		32	15	35.4	*Eoc/Oli*?
		16	18	B&R-18[e]	17	12	16.3	Bur/Lang
		5	3		5		5.2	*Mio/Pli*

[a] Ages shown in bold are from the studied area. Abbreviations: SE Gond.: Southeast Gondwana; SP: Super province; LIP: Large igneous province; STC: Short-term cycle; Tr: Triassic; J: Jurassic; Pli: Pliensbachian; Toa: Toarcian; Baj: Bajocian; Bat: Bathonian; Cal: Callovian; Oxf: Oxfordian; Cr: Cretaceous; Bar: Barremian; Apt: Aptian; Alb: Albian; Cen: Cenomanian;San: Santonian; Cam: Campanian; T: Tertiary; Pal: Paleocene; Eoc: Eocene; Lut: Lutetian; Bart: Bartonian; Oli: Oligocene; Bur: Burdigalian; Lang: Langhian; Mio: Miocene; Pli: Pliocene. Ont: Ontong Java oceanic plateau basalts; B&R: Basin and Range volcanism.

[b] Mesozoic geological boundaries after Gradstein et al. (1995) and Cenozoic geological boundaries after Harland et al. (1990); bold text: period boundary; italic text: epoch boundary; normal text: stage boundary.

[c] After Tarduno et al. (1991).

[d] Starting age of the Brito-Arctic event, North Atlantic Province, after Sinton et al. (1998).

[e] After Gans and Bohrson (1998).

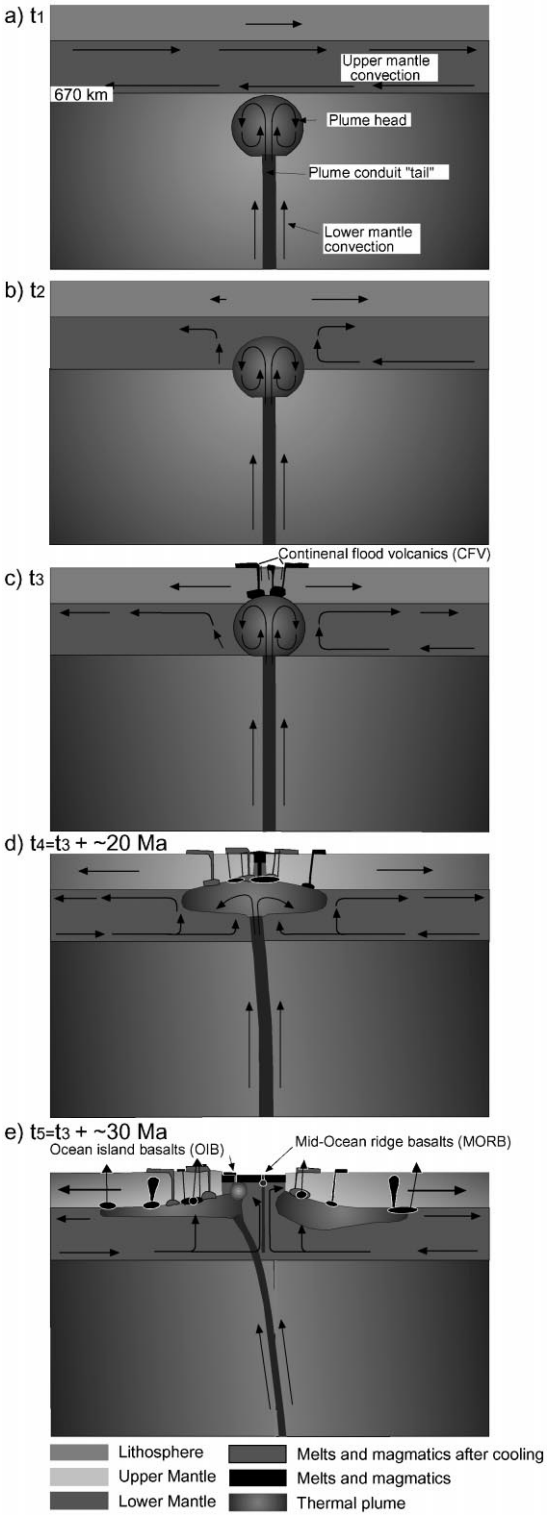

(Fig. 3, Table 3): 202, 190, 184, 169, 160, 145, 138, 125, 112, 97, 83, 69, 56, 44, 32, 17 and 5.

At present, and still under study, is the data set of 17 short-term magmatic cycles in Gondwana showing a large range of values (6–15 m.y.) averaging 12.3 m.y. (S.D. = 2.8), similar to that in the Levant alone (~13 m.y.). The global synchronous chronology of the high rates of upwelling convection in distal igneous provinces is probably due to upper mantle convection that, according to Olson et al. (1990), generated plate motions.

5.1. Dynamic evolution and consequences of episodic plume activity

It is likely that there is a strong link between mantle convection and crust formation via plume-driven magmatism and subduction-driven arc magmatism and accretion, and that large mantle plumes ascending from a thermal layer just above the core–mantle boundary are a result of lower mantle upwelling (Griffiths and Campbell, 1990; Olson et al., 1990). The penetration (Fig. 5a) of a large plume head

Fig. 5. Schematic diagram depicting a series of 'snapshots' of a cross-section beneath a plume province. The starting plume head evolution, which represents the ascent of a plume from the lower mantle, is based on laboratory experiments by Griffiths and Campbell (1990). (a) Plume, which originates close to the core–mantle boundary and rises up to the upper mantle, presumed to be as much as 800–1200 km in diameter. (b) Plume ascending across the 670 km discontinuity layer (lower–upper mantle boundary) and causing a major effect of stirring in the upper mantle convective cells. (c) Plume head reaching the lithosphere and causing thinning, uplifting, extension and fracturing (rifting) of the lithosphere, as well as producing an enormous amount of melt that ascends across the lithosphere to the Earth's surface as CFV or equivalents (a good example is the Afar plume between 31 and 20 m.y. ago at the time of the Yemen and Ethiopia CFV). Re-establishment of the upper mantle convection leads to initial divergent circulation. (d) Flattening and spreading of the plume head beneath the rigid lithosphere, approximately doubling its diameter to thousands of kilometers. The duration of this stage was ~20 m.y. when periodical igneous activity took place, while the vertical and horizontal velocities of the thermal plume decrease considerably. The beginning of significant divergent upper mantle circulation leads to continental breakup before the initiation of oceanic spreading center. (e) Stage in the process of oceanic spreading when the main driving force that lifts magmas across the lithosphere is upper mantle convection.

(~1000 km in diameter) and/or a few coexisting adjacent plume heads (Olson et al., 1988) into the upper mantle is presumed to cause major stirring in upper mantle convective cells (Griffiths and Campbell, 1990) (Fig. 5b), and therefore, it is suggested that it causes antithetical circulation in the upper mantle (Fig. 5c and d). Subsequently, the adjustment of this contradictory convection will produce divergent environments (Fig. 5d) of upper mantle convection cells that lead to continental extension, breakup, massive igneous activity, spreading and drifting. Hence, the upwelling lower mantle convection (plume discharge), relative to the sinking of the oceanic lithosphere at subduction zones, plays a major role in the continental dispersal process (plate tectonics).

The chronology of plumes over the last 205 m.y. presented herein (Fig. 3) indicates almost continuous upwelling of new lower mantle plumes with specific periods (enduring about 60 m.y.) of contemporaneous plume activity in a few plume provinces. Parts of these periods, such as the Cretaceous (124–83 Ma, according to Larson, 1991) and the Jurassic (~205–190 Ma, according to Algeo, 1996, and ~180–160 Ma, according to Larson, 1991, Fig. 3), are characterized by a geomagnetic normal-polarity superchron (Algeo, 1996), intensified global ocean-crust production, and an increase of eustatic sea level changes. Larson (1991) referred to each of these periods as a 'super-plume episode' when increasing convection in the outer core stopped the variations in geomagnetic field polarities and fuelled the super-plume eruptions. Stein and Hofmann (1994) related such periods to a strongly penetrative two-layer mantle convection caused by the descent of cold material from the 670 km discontinuity layer into the lower mantle, which in turn enhanced the rise of major plumes from the core–mantle boundary to the surface.

The present paper suggests that the duration of short-term magmatic cycles is ~13 m.y., as identified in the Tethyan super province, and strongly supported by similar information from other igneous provinces of Gondwana. The starting age of the magmatic events presumably represents an upper mantle systematic upwelling cycle that played a major role in the ascent of magmas across the lithosphere, and which suggests global synchronism (Fig. 3).

In addition to the importance of upwelling of lower mantle plumes for the ascent of melts across the lithosphere, it seems that the increase in upwelling energy by the upper mantle system is a critical factor in the ascent of magmas, particularly at the late stages of plume evolution (Fig. 5e). The duration and strength of specific magmatic events vary from place to place according to characteristics of the plume, upper mantle upwelling, and the lithosphere.

According to the suggested geochronological considerations, the presence of coexisting magmatic regimes (long-term lower mantle upwelling, and short-term upper mantle upwelling) is consistent with the two-layer convective model (Olson et al., 1990).

Vogt (1972) correlated mainly K–Ar data of Late Cretaceous and Tertiary plume volcanism and suggested the 'globally synchronous' model for plume convection. He also supported the correlation between the last four period boundaries and heightened plume volcanism. The present paper presents reliable age determinations that significantly decrease the range of the measured dates and strengthen Vogt's observation. Moreover, the high-resolution ages show 17 magmatic events marked by synchronism of greater or lesser extent, all of which fit well with either period or stage boundaries (Table 3, Fig. 3). These geological boundaries are marked by faunal crises, some of them by extinction crises (Sepkoski, 1990). It is therefore convincing that the world-wide plume activity, which is the cause of major magmatic/volcanic events, fluctuates with a globally periodic synchronous rhythm.

Acknowledgements

I wish to thank Y. Kolodny, M. McWilliams and H. Ron for their kind permission to publish their $^{40}Ar/^{39}Ar$ ages, and likewise, Z. Lewy and B. Lang for the K–Ar data. I also thank Y. Kapusta for his fruitful discussions, P. Kotlarsky for his assistance with the data processing and calculations, and B. Katz for editing the text. The paper benefited greatly from discussions and reviews of T. Weissbrod, M. Stein, M. Abelson and R. Weinberger. The paper was considerably improved by the comments of the anonymous reviewers.

Appendix A

Table A1
Summary of $^{40}Ar/^{39}Ar$ plateau ages and Rb/Sr isochron ages of magmatic rocks from Israel (all ages are in million years)[a]

Location	Sample number	Rock type	Pervious age (Ma)	Reinterpreted age (Ma)	Interpretation and reliability[b]	Source	Fig. 2
Heletz Deep-1	Rb/Sr	Rhyolite	*244* ± 44		Crystallization[c]	Steinitz (1980)	
SW Sinai	1190	Wr	240.3 ± 3.5	Unavailable	Crystallization[c]	Steinitz et al. (1992)	
SW Sinai	1187A	WR	266.2 ± 3.7	Unavailable	Crystallization[c]	Steinitz et al. (1992)	
SW Sinai	1183C	WR	273.6 ± 4.0	Unavailable	Crystallization[c]	Steinitz et al. (1992)	
Atlit-1	AD-90	WR basalt	193.3 ± 2.6	189.0 ± 2.6	Crystallization[d]	Kohn et al. (1993)	d
Atlit-1	AD-204	WR picrite	194.5 ± 3.4	190.3 ± 2.8	Heating[d]	Kohn et al. (1993)	
		Basalt	206.4 ± 3.8	–	Crystallization[c]		
Atlit-1	AD-225	WR gabbro	196.3 ± 2.8	190.9 ± 2.6	Cooling[e]	Kohn et al. (1993)	e
Atlit-1	AD-246	WR quartz	159.6 ± 2.2	161.0 ± 2.2	Heating[c]	Kohn et al. (1993)	c
		Keratophyre	206.8 ± 3.0	–	Crystallization[c]		
Atlit-1	AD-270	WR quartz Keratophyre	114.8 ± 1.7	109.2 ± 1.6	Heating[c]	Kohn et al. (1993)	
Atlit-1	AD-345		133.6 ± 1.9	132.0 ± 1.9	Heating[f]	Kohn et al. (1993)	f
Ramon, Saharon	RA-13b$_1$	WR basalt	209.1 ± 2.1	205 ± 2	Crystallization[d]	Baer et al. (1995)	a
Ramon, Saharon	RA-13b$_2$	WR basalt	210.0 ± 3.4	207 ± 3	Crystallization[d]	Baer et al. (1995)	b
Ramon, Ardon	23a	WR basalt	137.3 ± 0.2	137.9 ± 0.2	Crystallization[d]	Teutsch et al. (1996)	g
Ramon, Ardon	23b	WR basalt	138.2 ± 0.2	137.6 ± 0.3	Crystallization[d]	Teutsch et al. (1996)	h
Ramon, Laccol	Neg 5	WR trachyte	127.1 ± 1.5	124.9 ± 1.2	Crystallization[f]	Lang and Steinitz (1994)	i
Ramon, Gavnun	Neg 21	WR q. syenite	122.5 ± 1.3	124.4 ± 1.3	Crystallization[d]	Lang and Steinitz (1994)	j
Ramon, Gavnun	Rb/Sr	Syenite	*124* ± 13	–	Crystallization[f]	Lang et al. (1988)	
Har Arif	Rb/Sr	Syenite	*123* ± 9	–	Crystallization[f]	Lang et al. (1988)	
Ramon, Arod	M-184	Amphibole	108.6 ± 1.0	–	Crystallization[f]	Lang and Steinitz (1996)	k
Ramon, Arod	M-189	Amphibole	111.6 ± 1.1	–	Crystallization[f]	Lang and Steinitz (1996)	l
Ramon, Arod	M-175	WR basalt	111.4 ± 1.1	–	Crystallization[f]	Lang and Steinitz (1996)	
Ramon, Arod	HA-1	WR basalt	111.3 ± 1.1	–	Crystallization[f]	Lang and Steinitz (1996)	
Ramon, Arod	HA-3	WR basalt	–	111.3 ± 1.1	Crystallization[d]	Lang and Steinitz (1996)	
Ramon, Arod	HA-5	WR basalt	110.2 ± 1.1	–	Crystallization[d]	Lang and Steinitz (1996)	
Timna	AST 10	Amphibole	107.5 ± 1.1	–	Cooling[f]	Weissbrod et al. (unpubl.)	
Timna	AST 11	Biotite	107.8 ± 1.1	–	Cooling[f]	Weissbrod et al. (unpubl.)	
Timna	AST 12	Biotite	109.3 ± 1.1	–	Cooling[f]	Weissbrod et al. (unpubl.)	
Timna	AST 13	Biotite	107.8 ± 1.2	–	Cooling[f]	Weissbrod et al. (unpubl.)	
Lower Galilee	DM 393	WR basalt	5.1 ± 0.1	–	Crystallization[f]	Heimann et al. (1996)	
Lower Galilee	GS 175	WR basalt	5.1 ± 0.1	–	Crystallization[f]	Heimann et al. (1996)	
Lower Galilee	GS 222	WR basalt	5.2 ± 0.1	–	Crystallization[f]	Heimann et al. (1996)	
Korazim	AH 412	WR basalt	5.0 ± 0.1	–	Crystallization[f]	Heimann et al. (1996)	
Golan	DM 344	WR basalt	4.8 ± 0.1	–	Crystallization[d]	Heimann et al. (1996)	
Lower Galilee	DM 394	WR basalt	4.3 ± 0.1	–	Crystallization[f]	Heimann et al. (1996)	
Lower Galilee	GS 223	WR basalt	4.7 ± 0.1	–	Crystallization[f]	Heimann et al. (1996)	
Lower Galilee	DM 522	WR basalt	3.8 ± 0.1	–	Crystallization[f]	Heimann et al. (1996)	
Korazim	DM 479	WR basalt	3.5 ± 0.1	–	Crystallization[f]	Heimann et al. (1996)	
Golan	DM 544	WR basalt	3.5 ± 0.1	–	Crystallization[f]	Heimann et al. (1996)	
Western Galilee	GS 204	WR basalt	3.8 ± 0.1	–	Crystallization[f]	Heimann et al. (1996)	
Hula SH2	AH 1162	WR basalt	2.02 ± 0.11	1.87 ± 0.09	Crystallization[d]	Heimann (1990)	
Hula SHJ1	AH 1171	WR basalt	2.16 ± 0.28	–	Crystallization[d]	Heimann (1990)	
Ayyelet Hashahar	AH 1163	WR basalt	1.37 ± 0.39	1.46 ± 0.28	Crystallization[d]	Heimann (1990)	
Hula 1	AH 1051	WR basalt	0.95 ± 0.03	0.97 ± 0.03	Crystallization[f]	Heimann (1990)	
Golan	BRG/81/23	WR basalt	0.233 ± 0.003	–	Crystallization[f]	Féraud et al. (1988)	

[a] All ages are in million years. Most of the previous ages are interpreted by the quoted authors as plateaus. Note: $^{40}Ar/^{39}Ar$ ages in normal text; Rb/Sr isochron ages in italics.

[b] The credibility of each sample is according to the criteria mentioned in Section 2.

[c] Estimate age.

[d] Marginal and acceptable age.

[e] Maximum age.

[f] Reliable age.

Appendix B

Table B1
$^{40}Ar/^{39}Ar$ data for WR basalts (Kolodny and Ron; McWilliams and Ron, unpublished)[a]

Sample	Total fusion age	Weighted mean age	Percentage ^{39}Ar	Isochron age	MSWD	$^{40}Ar/^{36}Ar$ intercept
2Rak (S_{2-3})	94.0±1.5	96.9±0.1	57	96.9±0.2	0.86	283±5
3Muk (S_{2-4})	76.2±17.4	96.2±0.6	61	96.5±0.2	0.07	288±8
1Me (S_{2-2})	90.8±5.3	94.6±0.2	39	95.4±0.5	0.43	285±9
ME_{1-6} (S_{2-5})	14.58±0.23	14.86±0.04	30	15.01±0.13	1.07	307±5
ME_{55-60} (S_{2-9})	14.03±0.44	13.95±0.12	68	14.39±0.18	0.05	303±6
ME_{31-36} (S_{2-7})	12.77±0.63	14.94±0.10	46	14.88±0.18	0.35	297±4
NML-2	16.14±0.10	16.08±0.07	67			
NML-12	15.14±0.19	15.61±0.10	42			
NML-14	15.47±0.07	15.34±0.05	52			
NML-21	13.45±0.07	13.31±0.06	68			

[a] All ages are in millions of years. The weighted mean age having a commutative $^{39}Ar > 50\%$ is a plateau age, $^{39}Ar < 50\%$ is the 'marginal' or 'best estimate' age. MSWD: mean sum of weighted deviates (goodness of fit). Uncertainties are 1σ standard deviations (selected spectra in Fig. 2n–q).

Appendix C

Table C1
K/Ar data of three hornblende xenocrysts from the Bat Shelomo Senonian volcano, Carmel area (Lewy, Lang and Segev, unpublished)[a]

Sample number	$^{40}Ar_{rad}$ (ppb wt.)	$^{40}Ar_{rad}$ (%)	K (% wt)	Age (Ma)
BL-1001	5.451	93.2	1.650	83.1±1.7
BL-1001	5.745	92.1	1.650	80.7±1.6
BL-1002	5.468	92.8	1.680	81.9±1.7
BL-1002	5.418	90.8	1.680	81.1±1.6
AS-99-3a	5.390	95.4	1.610	84.3±1.7

[a] Decay and isotopic constants as suggested by Steiger and Jäger (1977).

Appendix D

Table D1
Geochronological data of the quoted magmatic events[a]

Location	Radiometric ages	Source
Central Atlantic		
Iberia & W Africa	Iberia: 204.7±2.5, 203.6±6.3, 198.8±1.7, 198±0.4; Morocco: 201.3, 197.6±2.4 197.1±1.8, 196.9±1.8; Algeria: 198±1.8; N. Mali: 203.7±2.7, 200.9±2.5, Northeast America: **201±1**	Sebai et al. (1991a)
Iberia	193±3	Bertrand (1991)
W Africa & N South America	French Guyana: 197.4±4.5, 196.2±1.7, 196.1±7.5, 196.0±4.5; 192.3±1.5, 189.0±1.2, Guinea: 201.4±1.5, 200.4±0.2, 200.2±2.4–188.7±1.9, 196±1, 194.8±0.5, 193.2±2.2	Deckart et al. (1997)
Liberia	191.3±3.4, 189.2±4.4	Dalrymple and Lanphere (1974)
Nigeria	*172*±5, *171*±2, *171*±5, *168*±5, *167*±2, *162*±2, *162*±3, *161*±4, *151*±4,	Reviewed by Cahen et al. (1984)
Benue Trough	146.7±1.6, 143.1±1.5	Maluski et al. (1995)

Table D1 *(continued)*.

Location	Radiometric ages	Source
N Brazil	~199, 198.3±1.0, 197.1±1.4, ~197, 191.1±0.4, 159.6±0.7, 159.0±0.6	Baksi and Archibald (1997)
Florida	*204*±20	Heatherington and Mueller (1991)
NE America	**200.9±1.0**, **201.3±1.0**	Dunning and Hodych (1990)
NE America	**202.0±1.06**, **201.4±0.81**	Hodych and Dunning (1992)
NE America	201.2±1.3, 199.3±3.0, 198.5±1.4, 198.4±6.1, 197.1±2.4, 196.0±2.8, 193.2±1.6, 189.6±2.2, 187.7±2.3	Sutter (1985)
Equatorial Atlantic		
Benue Trough	138.8±1.8. 137.8±1.9, 130.7±2.7, 123.1±1.6, 97.1±1.2, 95.3±1, 92.3±1.1, 87.7±1, 85.7±1.2, 84.4±1.2, 83.2±1.5, 83.1±1, 81.1±1.1, 74.3±1, 71.4±1.3, 68.4±1.1	Maluski et al. (1995)
	Guinea: *104.5*±1.6; South America : 83±6, 105±9,	Reviewed by Wilson and Guiraud (1998)
N Brazil	128, 124.9±0.9, 124.6±0.6, ~123	Baksi and Archibald (1997)
Paraná -Etendeka		
Paraná	132.8±1.1, 132.9±0.6, 132.6±0.3, 131.4±1.6, 132.7±1.2, 132.5±0.3, 132.4±0.7	Renne et al. (1992)
Paraná	138.4±1.3, 137.8±0.7, 137.4±1.0, 136.5±0.8, 135.6±1.5, 134.7±0.4, 134.2±2.0, 133.4±1.2, 133.1±0.6, 133.0±3.0, 132.8±1.8, 132.7±1.9, 132.6±2.2, 132.2±1.0, 131.8±1.2, 131.5±0.8, 129.1±1.4, 128.2±0.7, 127.2±1.2, 127.0±0.6 (isochron)	Stewart et al. (1996)
Paraná	131.4±0.5, 131.2±0.5, 131.0±0.5, 130.9±0.4, 130.7±0.4, 130.5±0.4, 130.5±0.6, 130.4±0.4, 130.2±0.4, 130.3±0.4, 129.2±0.4, 125.8±0.6, 120.8±0.7, 120.7±1.3	Renne et al. (1996)
Paraná	137.8±0.7, 137.2±1.1, 136.4±0.4, 134.1±0.4, 133.2±4.7, 132.3±0.8, 131.2±1.1, 129.4±1.3, 128.7±1.1, 127.7±4.6, 127.6±1.2, 126.8±2.0 (isochron)	Turner et al. (1994)
Paraná	134.5±0.4, 134.4±0.5, 134.0±0.3, 132.8±0.7, 130.6±0.2, 130.5±0.2, 130.4±0.2, 129.8±0.3, 129.4±0.3, 82.3±0.1, 81.8±1.8, 69.7±0.2	Deckart et al. (1998)
NE Paraná	83.7±0.8, 83.6±1.4, 83.4±0.8, 75.0±1.1 (K/Ar phlogopite)	Gibson et al. (1995)
NW Namibia	*129.1±2.0*, *128.6±1.0*, *128.5±1.5*, *127.4±24*, *126.3±1.0*, *123.4±1.4*	Milner et al. (1993)
W South Africa	*135*, *127*, *90*±3, *90*±3, *90*±3, *90*±4, *84*, *83*±4	Allsopp and Barrett (1975)
Angola	131.9±1.6, 131.6±1.4, 126.1±1.4, 95±2	Marzoli et al. (1999)
Karoo		
South Africa	*197±11*	Allsopp et al. (1984a)
South Africa	*191*±*9*, *175*±*7*, *145–140*	Allsopp et al. (1984b)
South Africa	*204*±*5*	Allsopp and Roddick (1984)
South Africa	200.8±4.5, 193.3±6.5, 191.1±8.0, 182.1±4.2, 181.9±5.2, 178.3±1.6, 145.8±1.3 (isochrons)	Hargraves et al. (1997)
South Africa	Lesotho: 186.5±1.9, 184.4±1.0, 184.3±1.7, 183.9±0.7, 183.9±1.0, 182.9±2.1, 182.4±1.7, 180.0±2.1, 179.5±2.1; Lebombo: 184.2±1.0, 184.2±0.6, 183.2±1.3, 182.7±0.8, 182.1±1.6, 181.2±1.0, 179.7±0.7, 178.1±0.6, 141.9±1.5; Transvaal: 182.8±1.6,181.4±1.1, 180.3±1.8; Namibia: 186.0±0.8, 184.2±1.0, 183.0±0.6, 181.5±0.8, 180.5±0.7	Duncan et al. (1997)
Antarctica	Kirwan Mt.: 182.8±0.6, 182.7±0.6, 180.6±0.6	Duncan et al. (1997)
Antarctica	Ferrar: 176.8±0.8, 176.5±0.5, 176.4±0.9, 175.9±0.5	Heimann et al. (1994)
Antarctica	Ferrar: 177.4±0.5, 177.2±0.5, 177.1±0.5, 176.9±0.5, 175.2±0.5, 174.9±0.5, 175.4±0.5	Elliot et al. (1999)
Antarctica	Ferrar: **183.8±1.6**, **183.6±2.1** South Africa: **183.7±0.6**	Encarnación (1996)
Antarctica	Dufek: **183.9±0.3**, **182.7±0.4**; 180.0±0.8, 178.1±1.1, 175.6±0.8 (hornblende)	Minor and Mukasa (1997)

Table D1 *(continued)*.

Location	Radiometric ages	Source
SE Australia	Victoria: **196±3**, **161±3**	Elburg and Soesoo (1999)
Ant. Peninsula	*195±21*, *176±8–173±3*	Millar and Pankhurst (1987)
Ant. Peninsula	*174±2*, *167±2*, *163±2*	Pankhurst (1982)
Ant. Peninsula	*156±6*, *152±8* (*Sm/Nd*), Milne, unpub. Ph.D. (1990): *176±4*, *160±4*	Millar et al. (1990)
Ant. Peninsula	144.6±3.6, **141±2**, 141±1, 140±4, 139.4±2.4 (Isochrons)	Vaughan et al. (1997, 1998)
Ant. Peninsula	**148–142 (Pb/Pb model age)**	Vaughan and Millar (1995)
Ant. Peninsula	**171±2**, **165±2**	Riley et al. (1998)
Ellsworth Land	**190**, **168±3**	Fanning and Laudon (1997)
Patagonia	*188±1*, *183±2*, *182±3*,*181±4*, *181±7*, *178±1*	Pankhurst et al. (1998)
Patagonia	156±2	Alric et al. (1996)
Patagonia	187.2±0.3, 187.4±0.6, 186.2±1.5, 186.3±0.3, 185.3±0.3, 182.7±0.3, 181.7±0.4, 181.6±0.3, 178.5±0.3, 178.5±0.9, 177.8±0.4, 177.0±0.8, 175.1±0.5, 168.6±0.4, 164.1±0.3, 158.4±0.3, 157.9±0.5, 154.6±0.5,153.4±0.3, 152.7±1.2, 152.8±2.6, 151.5±0.5, 147.1±0.5,144.2±0.4	Féraud et al. (1999)
SW India	144±6	Radhakrishna et al. (1999)
Indian		
Rajmahal	117.3±1.0, 117.0±0.3, 116.9±2.3, 115.5±1.3	Baksi (1995)
Rajmahal	126.4±2.8	Sakai et al. (1997)
	SW Australia (Bunbury): 130±0.5; Rajmahal: 115.7±0.6; Kerguelen: 110.1±0.6; India margins: 113.5±0.5; Antarctica margins: 112.1±0.5	Pringle et al. (1994)
SW Australia	Bunbury: 115±2	Colwell et al. (1994)
Madagascar	90.7±0.6, 89.1±0.6, 88.5±1.6, 885.8±1.1, 86.8±0.8, 86.0±1 (Plateau); 89.3±3.9, 87.6±2.9, 86.3±1.0, 86.3±1.9, 86.2±1.8, 84.8±1.3, 84.7±0.6, 84.5±0.7, 84.4±0.5, 83.7±5.0 (Isochron)	Storey et al. (1995)
Madagascar	83.6±1.6; **91.6±0.3**, **91.2±0.1**	Torsvik et al. (1998)
Deccan	67.6±1.8, 66.4±1.9, 65.1±0.6, 63.6±0.2, 63.6±0.5	Courtillot et al. (1988)
Deccan	68.57±0.08, 68.53±0.16, 64.96±0.11	Basu et al. (1993)
Deccan	67.5±0.6, 67.5±0.7, 67.0±0.8, 66.8±0.6, 66.8±0.6, 66.5±0.8, 66.1±0.8, 64.1±1.0, 62.4±0.8, 62.1±1.0	Venkatesan et al. (1993)
Deccan	66.3±0.7, 65.9±0.4, 65.6±0.6, 65.6±0.5, 65.1±0.6, ~65, 64.9±0.5, 64.7±1.1, 64.5±0.5, ~64, ~60.8±0.6	Baksi (1994)
SW India	144±6, 86.5±0.8, 70.2±1.4, 68.9±1.7, 68.0±2.2, 66.6±1.9, 61.0±2.7, 54.1±0.6	Radhakrishna et al. (1999)
Seychelles	*63.6±0.8*, *63.2±1.0*, *63.0±3.1*	Dickin et al. (1986)
Afar		
S Ethiopia	45.2±1.4, 39.8±0.8, 36.9±1.8, 36.3±1.5, 34.1±0.5, 19.1±0.3,17.0±0.3, 12.4±1.1	George et al. (1998)
S Ethiopia	37.2±0.07, 36.8±0.05, 36.8±0.05, 36.7±0.05 (sin.-crys. Senidine); 44.9±0.7, 42.5±0.7, 39.8±0.6, 37.9±0.6, 37.6±0.6, 37.0±0.6, 35.5±0.6, 33.9±0.5; 18.3±0.3, 13.7±0.2, 12.9±0.2; 1.34±0.03, 0.99±0.10, 0.77±0.03	Ebinger et al. (1993)
Ethiopian rift	6.69±0.02, 6.67±0.04, 5.64±0.13, 5.21±0.06, 5.17±0.02, 5.019±0.005, 5.00±0.01, 0.60±0.0205 (sin.-crys.feldspar from rhyolites)	Chernet et al. (1998)
N Ethiopia	31.1±0.6, 30.8±0.4, 30.6±0.1, 30.5±1.0, 30.4±0.4, 30±0.3, 29.6±0.3, 29.6±0.1, 29.5±0.2, 29.4±1.1, 28.8±0.6, 28.6±0.3, 28.2±0.1, 28.2±0.1, 26.7±0.1 (WR & mineral separates)	Hofmann et al. (1997)
N Ethiopia	30.1±0.1, 30.1±0.1, 29.7±0.05 (sanidine)	Rochette et al. (1998)
Republic of Djibouti	23.6±0.5, 19.0±0.3, 17.3±0.2, 16.7±0.4, 15.4±0.3, 11.8±0.6, 2.3±0.2, 1.00±0.09, 1.90±0.5, 1.54±0.7, 2.0±0.2, 0.25±0.02, 0.77±0.02, 1.03±0.03, 0.88±0.02 (WR & mineral separates)	Zumbo et al. (1995a)

Table D1 *(continued)*.

Location	Radiometric ages	Source
S Yemen	29.4±0.8, 28.9±0.1, 27.6±0.6, 26.5±0.4, 26.5±0.8, 25.4±0.1, 25.4±0.1, 24.9±0.8, 22.3±0.1, 21.4±0.1, 20.6±0.5, 18.5±0.6, 18.2±0.5, 16.1±0.9 (WR & mineral separates)	Zumbo et al. (1995b)
Yemen	30.7±0.3, 29.8±0.2, 29.6±0.6, 29.2±0.3, 28.9±0.2 (plagioclases); 30.4±0.2, 29.2±0.2, 19.7±0.6 (amphiboles); 29.3±0.1, 29.1±0.1, 29.1±0.2, 28.5±0.2, 28.2±0.1, 26.5±0.1 (anorthoclases); 28.2±0.1, 27.7±0.1, 26.9±0.2 (sanidines); 29.5±0.2 (biotite)	Baker et al. (1996)
Saudi Arabia	28.0±0.2, 27.2±0.2, 26.9±0.9, 24.5±1.3, 24.0±0.2, 23.3±0.5, 22.6±0.9, 22.50±0.06, 22.3±0.6, 22.2±1.1, 22.0±0.5, 22.0±0.3, 21.8±0.3, 21.7±0.3, 21.5±0.1, 21.25±0.05, 21.1±0.5, 21.1±0.2 (WR & mineral separates)	Sebai et al. (1991b)
Marie Byrd Land-Eastern Australia		
NE Australia	**132.5±2.4**, **130.8±3.4**, **119.3±2.2**; 145±3, 142±1.5, 135±3 (K/Ar hornblende), 139±1.4, 135±1.4, 134±1.4, 120±1.3, 117±1.2, 103±1 (K/Ar biotite), 106±1 (K/Ar K-spar)	Allen et al. (1998)
E Australia	Whitsunday volc. Prov.: *124*, *116*, *113*, *110*, *107*, *107*, *105* (from several sources)	Bryan et al. (1997)
Lord Howe Rise	94.8±1.3–93.4±0.7 (K/Ar); 96.1±2.2–89.4 ±1.2 (Ar/Ar total gas age)	McDougall and van der Lingen (1974)
New Zealand	**114–109**, **81.7±1.8**	Waight et al. (1998)
New Zealand	**101**	Muir et al. (1997)
Marie Byrd Land	102–95 (K/Ar biotite)	Reviewed by Weaver et al. (1994)
Marie Byrd Land	99	Palais et al. (1993)
Ant. Peninsula	133±5, 129±2, 127.1±2.5	Vaughan et al. (1997, 1998)
Balleny		
Soela Seamount	36 (from R.A. Duncan, 1992)	Lanyon et al. (1993)
Soela Seamount	31.5–33.4 (K/Ar from I. McDougall, 1988, 1992)	Lanyon et al. (1993)
NE Australia	~56, 44–42, 36–20, 18–16, 3–0.5 (K/Ar from several sources)	Reviewed by Griffin et al. (1987)

[a] All ages are in million years. Note: $^{40}Ar/^{39}Ar$ plateau ages in normal text (sin.-crys. = weighted means age single-crystal laser fusion; isochron = isochron age for $^{40}Ar/^{39}Ar$ step-heating analyses); K/Ar age = whole Rock (WR) or mineral age; U/Pb age in bold text; Rb/Sr or Sm/Nd isochron age in italics text.

References

Algeo, T.J., 1996. Geomagnetic polarity bias pattern through the Phanerozoic. J. Geophys. Res. 101, 2785–2814.

Allen, C.M., Williams, I.S., Stephens, C.J., Fielding, C.R., 1998. Granite genesis and basin formation in an extensional setting: the magmatic history of the northernmost New England Orogen. Aust. J. Earth Sci. 45, 875–888.

Allsopp, H.L., Barrett, D.R., 1975. Rb–Sr age determinations of South African kimberlite pipes. In: Ahrens, L. et al., (Eds.), Physics and Chemistry of the Earth Vol. 9, 605 pp.

Allsopp, H.L., Roddick, J.C., 1984. Rb–Sr and ^{40}Ar–^{39}Ar age determination on phlogopite micas from the pre-Lebombo Group Dokolwayo kimberlite pipe. Spec. Publ. Geol. Soc. S. Afr. 13, 267–271.

Allsopp, H.L., Bristow, J.W., Logan, C.T., Eales, H.V., Erlank, A.J., 1984a. Rb–Sr geochronology of three Karoo-related intrusive complexes. Spec. Publ. Geol. Soc. S. Afr. 13, 218–287.

Allsopp, H.L., Manton, W.I., Bristow, J.W., 1984b. Rb–Sr geochronology of Karoo felsic volcanics. In: Erlank, A.J. (Ed.), Petrogenesis of the Volcanic Rocks of the Karoo Province. Spec. Publ. Geol. Soc. S. Afr. 13, 273–280.

Alric, V.I., Haller, M.J., Féraud, G., Bertrand, H., Zubia, M., 1996. Cronología $^{40}Ar/^{39}Ar$ del vulcanismo jurásico de la Patagonian extraandina, Actas del XIII Congreso Geológico Argentino, Buenos Aires, Tomo Vol. 5., 243–250.

Anderson, D.L., 1994a. Superplumes or supercontinents? Geology 22, 39–42.

Anderson, D.L., 1994b. The sublithospheric mantle as the source of continental flood basalts, the case against the continental lithosphere and plume head reservoirs. Earth Planet. Sci. Lett. 123, 269–280.

Baer, G., Heimann, A., Eshet, Y., Weinberger, R., Mussett, A., Sherwood, G., 1995. The Saharonim basalt: A Late Triassic–Early Jurassic intrusion in southeastern Makhtesh Ramon, Israel. Isr. J. Earth Sci. 44, 1–10.

Baker, J., Snee, L., Menzies, M., 1996. A brief Oligocene period

of flood volcanism in Yemen: Implication for the duration and rate of continental flood volcanism at the Afro-Arabian triple junction. Earth Planet. Sci. Lett. 138, 39–55.

Baksi, A.K., 1994. Geochronological studies on whole-rock basalts, Deccan Traps, India: Evaluation of the timing of volcanism relative to the K–T boundary. Earth Planet. Sci. Lett. 121, 43–56.

Baksi, A.K., 1995. Petrogenesis and timing of volcanism in the Rajmahal flood basalt province, northeastern India. Chem. Geol. 121, 73–90.

Baksi, A.K., 1999. Reevaluation of plate motion models based on hotspot tracks in the Atlantic and Indian oceans. J. Geol. 107, 13–26.

Baksi, A.K., Archibald, D.A., 1997. Mesozoic igneous activity in the Maranhão province, northern Brazil: $^{40}Ar/^{39}Ar$ evidence for separate episodes of basaltic magmatism. Earth Planet. Sci. Lett. 151, 139–153.

Basu, A.R., Renne, P.R., DasGupta, D.K., Teichmann, F., Poreda, R.J., 1993. Early and late alkali igneous pulses and a high-^{3}He plume origin for the Deccan flood basalts. Science 261, 902–905.

Bertrand, H., 1991. The Mesozoic tholeiitic provinces of northwest Africa: A volcano-tectonic record of the early opening of Central Atlantic magmatism in extensional structural setting. In: Kampunzu, A.B., Lubala, R.T. (Eds.), The Phanerozoic African Plate. Springer, Berlin, pp. 147–188.

Bryan, S.E., Constantine, A.E., Stephens, C.J., Ewart, A., Schön, R.W., Parianos, J., 1997. Early Cretaceous volcanosedimentary successions along the eastern Australian continental margin: Implications for the break-up of eastern Gondwana. Earth Planet. Sci. Lett. 153, 85–102.

Cahen, L., Snelling, N.J., Delhal, J., Bonhomme, M., Ledent, D., 1984. The Geochronology and Evolution of Africa. Clarendon Press, Oxford.

Chernet, T., Hart, W.K., Aronson, J.L., Walter, R.C., 1998. New age constraints on the timing of volcanism and tectonism in the northern main Ethiopian rift–southern Afar transition zone (Ethiopia). J. Volcanol. Geotherm. Res. 80, 267–280.

Coffin, M.F., Eldholm, O., 1994. Large igneous provinces: Crustal structure, dimensions, and external consequences:. Rev. Geophys. 32, 1–36.

Colwell, J.B., Symonds, P.A., Crawford, A.J., 1994. The nature of the Wallaby (Cuvier) Plateau and other igneous provinces of the West Australian margin. In: Neville, E. (Ed.), Geology of the Outer North West Shelf, Australia. AGSO J. Austr. Geol. Geophys. 15 (1), 137–156.

Courtillot, V., Féraud, G., Maluski, H., Vandamme, D., Moreau, M.G., Besse, J., 1988. Deccan flood basalts and the Cretaceous/Tertiary boundary. Nature 333, 843–846.

Cox, K.G., 1989. The role of mantle plumes in the development of continental drainage patterns. Nature 342, 873–877.

Dalrymple, G.B., Lanphere, M.A., 1974. $^{40}Ar/^{39}Ar$ age spectra of some undisturbed terrestrial samples. Geochim. Cosmochim. Acta 38, 715–738.

Deckart, K., Féraud, G., Bertrand, H., 1997. Age of Jurassic continental tholeites of French Guyana, Surinam and Guinea: Implications for the initial opening of the Central Atlantic Ocean. Earth Planet. Sci. Lett. 150, 205–220.

Deckart, K., Féraud, G., Marques, L.S., Bertrand, H., 1998. New time constraints on dyke swarms related to the Paraná–Etendeka magmatic province and subsequent South Atlantic opening, southeastern Brazil. J. Volcanol. Geotherm. Res. 80, 67–83.

Dickin, A.P., Fallick, A.E., Halliday, A.N., Macintyre, R.M., Stephens, W.E., 1986. An isotopic and geochronological study of the younger igneous rocks of the Seychelles. Earth Planet. Sci. Lett. 81, 46–56.

Duncan, R.A., Hooper, P.R., Rehacek, J., Marsh, J.S., Duncan, A.R., 1997. The timing and duration of the Karoo igneous event, southern Gondwana. J. Geophys. Res. 102, 18127–18138.

Dunning, G.R., Hodych, J.P., 1990. U/Pb zircon and baddeleyite ages for the Palisades and Gettysburg sills of the northeastern United States: Implications for the age of the Triassic/Jurassic boundary. Geology 18, 795–798.

Ebinger, C.J., Yemane, T., WoldeGabriel, G., Aronson, J.L., Walter, R.C., 1993. Late Eocene–Recent volcanism and faulting in the southern main Ethiopian rift. Geol. Soc. Lond. J. 150, 99–108.

Elburg, M.A., Soesoo, A., 1999. Jurassic alkali-rich volcanism in Victoria (Australia): lithospheric versus asthenospheric source. J. Afr. Earth Sci. 29, 269–280.

Elliot, D.H., Fleming, T.H., Kyle, P.R., Foland, K.A., 1999. Long-distance transport of magmas in the Jurassic Ferrar large igneous province, Antarctica. Earth Planet. Sci. Lett. 167, 89–104.

Encarnación, J., Fleming, T.H., Elliot, D.H., Eales, H.V., 1996. Synchronous emplacement of Ferrar and Karoo dolerites and the early breakup of Gondwana. Geology 24, 535–538.

Fanning, C.M., Laudon, T.S., 1997. Mesozoic volcanism and sedimentation in eastern Ellsworth Land, West Antarctica, Conflicting evidence for arc migration? Geol. Soc. Am. Prog. 29, A51517.

Féraud, G., Alric, V., Fornari, M., Bertrand, H., Haller, M., 1999. $^{40}Ar/^{39}Ar$ dating of the Jurassic volcanic province of Patagonia: migrating magmatism related to Gondwana break-up and subduction. Earth Planet. Sci. Lett. 172, 83–96.

Féraud, G., York, D., Hall, C.M., Goren, N., Schwarcz, H.P., 1988. $^{40}Ar/^{39}Ar$ age limit for an Acheulian site in Israel. Nature 304, 263–265.

Führmann, U., Hess, J.C., Lippolt, H.J., 1986. HD-B1: a potential standard for K–Ar chronometrym. Mitt. Lab. Geochron. Univ. Heidelberg 209, 1–3.

Gans, P.B., Bohrson, W.A., 1998. Suppression of volcanism during rapid extension in Basin and Range province, United States. Science 279, 66–68.

Garfunkel, Z., 1989. Tectonic setting of Phaneorozoic magmatism in Israel. Isr. J. Earth Sci. 38, 51–74.

George, R., Rogers, N., Kelley, S., 1998. Earliest magmatism in Ethiopia: Evidence for two mantle plumes in one flood basalts province. Geology 26 (10), 923–926.

Gibson, S.A., Thompson, R.N., Leonardos, O.H., Dickin, A.P.,

Mitchell, J.G., 1995. The Late Cretaceous impact of the Trindade mantle plume: evidence from large-volume, mafic, potassic magmatism in SE Brazil. J. Petrol. 36, 189–229.

Gradstein, F.M., Agterberg, F.P., Ogg, J.G., Hardenbol, J., Veen, P.V., Thierry, J., Huang, Z., 1995. A Triassic, Jurassic and Cretaceous time scale. In: Berggren, W.A., Kent, D.V., Aubry, M.P., Hardenbol, J. (Eds.), Geochronology, Time Scales and Global Stratigraphic Correlation. Soc. Sedim. Geol. Spec. Publ. 54, 95–126.

Griffin, W.L., Sutherland, F.L., Hollis, J.D., 1987. Geothermal profile and crust–mantle transition beneath east-central Queensland: Volcanology, xenolith petrology and seismic data. J. Volcanol. Geotherm. Res. 31, 177–203.

Griffiths, R.W., Gurnis, M., Eitelberg, G., 1989. Holographic measurements of surface topography in laboratory models of mantle hotspots. Geophys. J. 96, 477–495.

Griffiths, R.W., Campbell, I.H., 1990. Stirring and structure in mantle starting plumes. Earth Planet. Sci. Lett. 99, 66–78.

Hargraves, R.B., Rehacek, J., Hooper, P.R., 1997. Palaeomagnetism of the Karoo igneous rocks in southern Africa. S. Afr. J. Geol. 100, 195–212.

Harland, W.B., Armstrong, R.L., Cox, A.V., Craig, L.E., Smith, A.G., Smith, D.G., 1990. A Geologic Time Scale 1989. Cambridge University Press, Cambridge.

Heatherington, A.L., Mueller, P.A., 1991. Geochemical evidence for Triassic rifting in southwestern Florida. Tectonophysics 188, 291–302.

Heimann, A., 1990. The Development of the Dead Sea Rift and its Margins in Northern Israel During the Pliocene and the Pleistocene. Geol. Surv. Isr. Rep. GSI/28/90. in Hebrew, English abstract, 114 pp.

Heimann, A., Steinitz, G., Zafrir, H., 1992. Irradiation of samples for $^{40}Ar/^{39}Ar$ dating using the Soreq Nuclear Research Center IRR-1 reactor, Israel. Nucl. Geophys. 6, 273–286.

Heimann, A., Fleming, T.H., Elliot, D.H., Foland, K.A., 1994. A short interval of Jurassic continental flood basalt volcanism in Antarctica as demonstrated by $^{40}Ar/^{39}Ar$ geochronology. Earth Planet. Sci. Lett. 121, 19–41.

Heimann, A., Steinitz, G., Mor, D., Shaliv, G., 1996. The Cover Basalt Formation, its age and its regional and tectonic setting: Implication from K–Ar and $^{40}Ar/^{39}Ar$ geochronology. Isr. J. Earth Sci. 45, 55–71.

Hodych, J.P., Dunning, G.R., 1992. Did the Manicouagan impact trigger end-of-Triassic mass extinction? Geology 20, 51–54.

Hofmann, C., Courtillot, V., Féraud, G., Rochette, P., Yirgu, G., Ketefo, E., Pik, R., 1997. Timing of the Ethiopian flood basalts event and implications for plume birth and global change. Nature 389, 838–841.

Huneke, J.C., Smith, S.P., 1976. The realities of recoil: ^{39}Ar recoil out of small grains and anomalous pattern in $^{40}Ar/^{39}Ar$ dating. Geochim. Cosmochim. Acta 7 Suppl., 1987–2008.

Izett, G.A., Dalrymple, G.B., Snee, L.W., 1991. $^{40}Ar/^{39}Ar$ age of Cretaceous–Tertiary boundary tektites from Haiti. Science 252, 1539–1542.

Kapusta, Y., Steinitz, G., Kotlarsky, P., 1994. Determination of the effective neutron flux for $^{40}Ar/^{39}Ar$ dating of fine-grained clay minerals. In: Lanphere, M.A., Dalrymple, G.B., Turrin, B.D. (Eds.), 8th International Conference on Geochronology Cosmochronology and Isotope Geology. US Geol. Surv. Circ. 1107, 162.

Kent, R.W., 1994. Superplumes or supercontinents? Comment. Geology 22, 1054–1055.

Kohn, B.P., Lang, B., Steinitz, G., 1993. $^{40}Ar/^{39}Ar$ dating of the Atlit-1 volcanic sequence, northern Israel. Isr. J. Earth Sci. 42, 17–28.

Lang, B., Hebeda, E.H., Priem, H.N.A., 1988. K–Ar and Rb–Sr ages of Early Cretaceous magmatic rocks from Makhtesh Ramon, southern Israel. Isr. J. Earth Sci. 37, 65–72.

Lang, B., Steinitz, G., 1989. K–Ar dating of Mesozoic magmatic rocks in Israel: A review. Isr. J. Earth Sci. 38, 89–103.

Lang, B., Steinitz, G., 1994. New $^{40}Ar/^{39}Ar$ dating of Early Cretaceous intrusive magmatics in Makhtesh Ramon. Geol. Surv. Isr. Curr. Res. 9, 37–40.

Lang, B., Steinitz, G., 1996. $^{40}Ar/^{39}Ar$ dating of Early Cretaceous basalts in Har Arod, Makhtesh Ramon. Geol. Surv. Isr. Curr. Res. 10, 106–110.

Lanyon, R., Varne, R., Crawford, A.J., 1993. Tasmanian Tertiary basalts, the Balleny plume, and opening of the Tasman Sea (southwest Pacific Ocean). Geology 21, 555–558.

Larson, R.L., 1991. Geological consequences of superplumes. Geology 19, 963–966.

McDougall, I., van der Lingen, G.J., 1974. Age of the rhyolites of the Lord Howe Rise and the evolution of the southeast Pacific Ocean. Earth Planet. Sci. Lett. 21, 117–126.

Maluski, H., Coulon, C., Popoff, M., Baudin, P., 1995. $^{40}Ar/^{39}Ar$ chronology, petrology and geodynamic setting of Mesozoic to early Cenozoic magmatism from the Benue Trough, Nigeria. J. Geol. Soc. Lond. 152, 311–326.

Marzoli, A., Melluso, L., Morra, V., Renne, P.R., Sgrosso, I., Dantonio, M., Duarte Morais, L., Morais, E.A.A., Ricci, G., 1999. Geochronology and petrology of Cretaceous basaltic magmatism in the Kwanza basin (western Angola) and relationships with the Paranà-Etendeka continental flood basalt province. J. Geodynam. 28, 341–356.

Millar, I.L., Pankhurst, R.J., 1987. Rb–Sr geochronology of the region between the Antarctic Peninsula and the Transantarctic Mountains: Haag Nunataks and Mesozoic granitoids. In: McKenzie, G.D. (Ed.), Gondwana Six: Structure, Tectonics and Geophysics. Am. Geophys. Union, Geophys. Monogr. 40, 151–160.

Millar, I.L., Milne, A.J., Whitham, A.G., 1990. Implications of Sm–Nd garnet ages for the stratigraphy of northern Graham Land, Antarctic Peninsula. Zentrablatt für Geologie und Paläeontologie, Teil., 97–104.

Milner, S.C., Le Roex, A.P., Watkins, R.T., 1993. Rb–Sr age determinations of rocks from the Okenyenya igneous complex, northwestern Namibia. Geol. Mag. 130, 335–343.

Minor, D.R., Mukasa, S.B., 1997. Zircon U–Pb and hornblende $^{40}Ar–^{39}Ar$ ages for the Dufek layered mafic intrusion, Antarctica: Implications for the age of the Ferrar large igneous province. Geochim. Cosmochim. Acta 61, 2497–2504.

Mor, D., 1986. The Volcanism of the Golan Heights, Geol. Surv. Isr. Rep. GSI/5/86. in Hebrew, English abstract, 159 pp.

Morgan, W.J., 1971. Convection plumes in the lower mantle. Nature 230, 42–43.

Morgan, W.J., 1981. Hotspot tracks and the opening of the Atlantic and Indian oceans. In: Emiliani, C. (Ed.), The Sea. Wiley, New York, pp. 443–487.

Muir, R.J., Ireland, T.R., Weaver, S.D., Bradshaw, J.D., Waight, T.E., Jongens, R., Eby, G.N., 1997. SHRIMP U–Pb geochronology of Cretaceous magmatism in NW Nelson-Westland, South Island, New Zealand. N.Z. J. Geol. Geophys. 40, 453–464.

Mutter, J.C., Buck, W.R., Zehnder, C.M., 1988. Convective partial melting 1. A model for the formation of thick basaltic sequences during the initiation of spreading. J. Geophys. Res. 93 B2, 1031–1048.

Olson, P., Schubert, G., Anderson, C., Goldman, P.J., 1988. Plume formation and lithosphere erosion: A comparison of laboratory and numerical experiments. J. Geophys. Res. 93 B12, 15065–15084.

Olson, P., Silver, P.G., Carlson, R.W., 1990. The large-scale structure of convection in the Earth's mantle. Nature 344, 209–215.

Palais, D.G., Mukasa, S.B., Weaver, S.D., 1993. U–Pb and $^{40}Ar/^{39}Ar$ geochronology for plutons along the Ruppert and Hobbs Coasts, Marie Byrd Land, west Antarctica: Evidence for rapid transition from arc to rift-related magmatism. EOS (Trans. Am. Geophys. Union) 74, 123.

Pankhurst, R.J., 1982. Rb–Sr geochronology of Graham Land, Antarctica. J. Geol. Soc. Lond. 139, 701–711.

Pankhurst, R.J., Leat, P.T., Sruoga, P., Rapela, C.W., Marquez, M., Storey, B.C., Riley, T.R., 1998. The Chon Aike province of Patagonia and related rocks in West Antarctica: A silicic large igneous province. J. Volcanol. Geotherm. Res. 81, 113–136.

Pringle, M.S., Storey, M., Wijbrans, J., 1994. $^{40}Ar/^{39}Ar$ geochronology of mid-Cretaceous Indian Ocean basalts: Constraints on the origin of large flood basalt provinces, In: Fall Meet. Suppl., San Francisco, Eos Trans. AGU 75, 728.

Radhakrishna, T., Maluski, H., Mitchell, J.T., Joseph, M., 1999. $^{40}Ar/^{39}Ar$ and K/Ar geochronology of the dykes from the south Indian granulite terrain. Tectonophysics 304, 109–129.

Recanati, P., Steinitz, G., Platzner, I., Starinsky, A., 1989. Early Cretaceous igneous activity in the northern Negev: evidence from K–Ar dating of subsurface cores:. Isr. J. Earth Sci. 38, 155–162.

Renne, P.R., Deckart, K., Ernesto, M., Féraud, G., Piccirillo, E.M., 1996. Age of the Ponta Grossa dike swarm (Brazil), and implications to Paraná flood volcanism. Earth Planet. Sci. Lett. 144, 199–211.

Renne, P.R., Ernesto, M., Pacca, I.G., Coe, R.S., Glen, J.M., Prévot, M., Perrin, M., 1992. The age of Paraná flood volcanism, rifting of Gondwanaland and the Jurassic–Cretaceous boundary. Science 258, 975–979.

Ribe, N.M., Christensen, U.R., 1994. Three-dimensional modeling of plume–lithosphere interaction. J. Geophys. Res. 99 B1, 669–682.

Riley, T.R., Crame, J.A., Thomson, M.R.A., Cantrill, D.J., 1998. Late Jurassic (Kimmeridgian-Tithonian) macrofossil assemblage from Jason Peninsula, Graham Land: evidence for a significant northward extention of the Latady Formation. Antarctic Sci. 9, 434–442.

Rochette, P., Tamrat, E., Féraud, G., Pik, R., Courtillot, V., Ketefo, E., Coulon, C., Hoffmann, C., Vandamme, D., Yirgu, G., 1998. Magnetostratigraphy and timing of the Oligocene Ethiopian traps. Earth Planet. Sci. Lett. 164, 497–510.

Roddick, J.C., 1983. High precision intercalibration of $^{40}Ar/^{39}Ar$ standards. Geochim. Cosmochim. Acta 47, 887–898.

Sakai, H., Funaki, M., Sato, T., Takigami, Y., Sakai, H., Hirooka, K., 1997. Paleomagnetic study with $^{40}Ar/^{39}Ar$ dating of Rajmahal hills and Mahanadi graben in India — reconstruction of Gondwanaland. J. Geol. Soc. Jpn. 103, 192–202.

Schilling, J.G., Kingsley, R.H., Hanan, B.B., McCully, B.L., 1992. Nd–Sr–Pb isotopic variations along the Golf of Aden: Evidence for Afar mantle plume–continental lithosphere interaction. J. Geophys. Res. 97 B7, 10927–10966.

Sebai, A., Féraud, G., Bertrand, H., Hanes, J., 1991a. $^{40}Ar/^{39}Ar$ dating and geochemistry of tholeiitic magmatism related to the early opening of the Central Atlantic rift. Earth Planet. Sci. Lett. 104, 455–472.

Sebai, A., Zumbo, V., Féraud, G., Bertrand, H., Hussain, A.G., Giannérini, G., Campredon, R., 1991b. $^{40}Ar/^{39}Ar$ dating of alkaline and tholeiitic magmatism of Saudi Arabia related to the early Red Sea rifting. Earth Planet. Sci. Lett. 104, 473–487.

Segev, A., 1998. Magmatic cyclicity in the Afro-Arabian Plate: Mantle convection generated. ICOG-9 (Abstr.), Beijing. Chin. Sci. Bull. 43, 115.

Segev, A., 1999. The control of mantle plume activity on the lithostratigraphy of Israel, Isr. Geol. Soc. Annu. Meet., Dead Sea, 79–80.

Sengör, A.M., Yilmaz, Y., Sungurlu, O., 1984. Tectonics of the Mediterranean Cimmerides: nature and evolution of the western termination of Palaeo-Tethys. In: Dixon, J.E., Robertson, A.H.F. (Eds.), The geological evolution of the eastern Mediterranean. Geol. Soc. Lond., Spec. Publ. 17, 77–112.

Sepkoski Jr., J.J., 1990. The taxonomic structure of periodic extinction: Global Catastrophes in Earth History. In: Sharpton, V.L., Ward, P.D. (Eds.), An Interdisciplinary Conference on Impacts, Volcanism and Mass Mortality. Geol. Soc. Am. Spec. Pap. 247, 33–44.

Sinton, C.W., Hitchen, K., Duncan, R.A., 1998. ^{40}Ar–^{39}Ar geochronology of silicic and basic volcanic rocks on the margins of the North Atlantic. Geol. Mag. 135, 161–170.

Steiger, R.H., Jäger, E., 1977. Subcommission on geochronology: Convention on the use of decay constants in geo- and cosmochronology. Earth Planet. Sci. Lett. 36, 359–362.

Stein, M., Hofmann, A.W., 1992. Fossil plume head beneath

the Arabian lithosphere? Earth Planet. Sci. Lett. 114, 193–209.
Stein, M., Hofmann, A.W., 1994. Mantle plumes and episodic crustal growth. Nature 372, 63–68.
Steinitz, G., Bartov, Y., Hunziker, J.C., 1978. K–Ar determination of some Miocene–Pliocene basalts in Israel: Their significance to the tectonics of the Rift Valley. Geol. Mag. 115, 329–340.
Steinitz, G., 1980. In: Rb–Sr Age Determination on Basement Rocks from Heletz Deep 1A Well. Geol. Sur. Isr. Rep. MM/1/80.
Steinitz, G., Bartov, Y., Eyal, M., 1992. K–Ar and Ar–Ar dating of Permo-Triassic magmatism in Sinai and Israel — initial results, Isr. Geol. Soc. Annu. Meet. Ashqelon (Abst.), 147–148.
Stewart, K., Turner, S., Kelley, S., Hawkesworth, C., Kirstein, L., Mantovani, M., 1996. 3-D ^{40}Ar–^{39}Ar geochronology in the Paraná continental flood basalt province. Earth Planet. Sci. Lett. 143, 95–109.
Storey, B.C., Mahoney, J.J., Saunders, A.D., Duncan, R.A., Kelley, S.P., Coffin, M.F., 1995. Timing of hot spot-related volcanism and the breakup of Madagascar and India. Science 267, 852–855.
Sutter, J.F., 1985. Progress on geochronology of Mesozoic diabases and basalts. In: Workshop on the Early Mesozoic Basins of the Eastern United States. Proc. 2nd US Geol. Surv. Circ. 946, 110–114.
Tarduno, J.A., Slitter, W.V., Kroenke, L., Leckie, M., Mayer, H., Mahoney, J.J., Musgrave, R., Storey, M., Winterer, E.L., 1991. Rapid formation of Ontong Java Plateau by Aptian mantle plume volcanism. Science 254, 399–403.
Teutsch, N., Ayalon, A., Kolodny, Y., 1996. Late Cretaceous exposure and paleoweathering of a basaltic dike, Makhtesh Ramon, Israel: Geochemical and stable isotope studies. Isr. J. Earth Sci. 45, 19–30.
Torsvik, T.H., Tucker, R.D., Ashwal, L.D., Eide, E.A., Rakotosolofo, N.A., de Wit, M.J., 1998. Late Cretaceous magmatism in Madagascar: paleomagnetic evidence for a stationary Marion hotspot. Earth Planet. Sci. Lett. 164, 221–232.
Turcotte, D.L., Schubert, G., 1982. Geodynamics. Applications of Continuum Physics to Geological Problems. Wiley, New York, 450 pp.
Turner, G., Cadogan, P.H., 1974. Possible effect of ^{39}Ar recoil in ^{40}Ar–^{39}Ar dating, Proc. 5th Lunar Sciences Conf. Geochim. Cosmochim. Acta 5, Suppl., 1601–1615.
Turner, S., Regelous, M., Kelley, S., Hawkesworth, C., Mantovani, M., 1994. Magmatism and continental break-up in the South Atlantic: High precision ^{40}Ar–^{39}Ar geochronology. Earth Planet. Sci. Lett. 121, 333–348.
Vaughan, A.P.M., Millar, I.L., 1995. Early Cretaceous magmatism during extentional deformation within the Antarctic Peninsula magmatic arc. J. S. Am. Earth Sci. 9, 121–129.
Vaughan, A.P.M., Wareham, C.D., Millar, I.L., 1997. Granitoid pluton formation by spreading of continental crust: the Wiley Glacier complex, northwest Palmer Land, Antarctica. Tectonophysics 283, 35–60.
Vaughan, A.P.M., Wareham, C.D., Johnson, A.C., Kelley, S.P., 1998. A Lower Cretaceous, syn-extensional magmatic anomalies: The Pacific Margin Anomaly (PMA), western Palmer Land, Antarctica. Earth Planet. Sci. Lett. 158, 143–155.
Venkatesan, T.R., Pande, K., Goplan, K., 1993. Did Deccan volcanism pre-date the Cretaceous/Tertiary transition? Earth Planet. Sci. Lett. 119, 181–189.
Vogt, P.R., 1972. Evidence for global synchronism in mantle plume convection and possible significance for geology. Nature 240, 338–342.
Waight, T.E., Weaver, S.D., Muir, R.J., 1998. Mid-Cretaceous granitic magmatism during the transition from subduction to extension in southern New Zealand: a chemical and tectonic synthesis. Lithos 45, 469–482.
Weaver, S.D., Storey, B.C., Pankhurst, R.J., Mukasa, S.B., DiVenere, V.J., Bradshaw, J.D., 1994. Antarctica–New Zealand rifting and Marie Byrd Land lithospheric magmatism linked to ridge subduction and mantle plume activity. Geology 22, 811–814.
White, R., McKenzie, D., 1989. Magmatism at rift zones: The generation of volcanic continental margins and flood basalts. J. Geophys. Res. 94, 7685–7729.
Wilson, T.J., Grunow, A.M., Hanson, R.E., 1996. Gondwana assembly: The view from southern Africa and east Gondwana. J. Geodynam. 23, 263–286.
Wilson, M., Guiraud, R., 1998. Late Permian to Recent magmatic activity on the African–Arabian margin of Tethys. In: MacGregor, D.S., Moody, R.T.J., Clark-Lowes, D.D. (Eds.), Petroleum Geology of North Africa. Geol. Soc. Lond., Spec. Publ. 132, 231–263.
Zeyen, H., Volker, F., Wehrle, V., Fuchs, K., Sobolev, S.V., Altherr, R., 1997. Styles of continental rifting: Crust–mantle detachment and mantle plumes. Tectonophysics 278, 329–352.
Zumbo, V., Féraud, G., Vellutini, P., Piguet, P., Vincent, J., 1995a. First $^{40}Ar/^{39}Ar$ dating on Early Pliocene to Plio-Pleistocene magmatic events of the Afar — Republic of Djibouti. J. Volcanol. Geotherm. Res. 65, 281–295.
Zumbo, V., Féraud, G., Bertrand, H., Chazot, G., 1995b. $^{40}Ar/^{39}Ar$ chronology of Tertiary magmatic activity in Southern Yemen during the early Red Sea–Aden rifting. J. Volcanol. Geotherm. Res. 65, 265–279.